A PHOTOGRAPHIC STUDY OF THE MECHANISM OF SURFACE BOILING AT ATMOSPHERIC PRESSURE

PARKER OLIN CHAPMAN
NORMAN FRED GEER

A PHOTOGRAPHIC STUDY OF THE MECHANISM OF SURFACE BOILING AT ATMOSPHERIC PRESSURE

By

Parker Olin Chapman
Lieutenant, U.S. Coast Guard
B.S., U.S. Coast Guard Academy, 1944

Norman Fred Geer
Lieutant, (j.g.), U.S. Navy
B.S., U.S. Naval Academy, 1945

Submitted in Partial Fulfillment of
the Requirements for the degree of

NAVAL ENGINEER

from the

MASSACHUSETTS INSTITUTE OF TECHNOLOGY

1951

C38

ABSTRACT

A. Title: A Photographic Study of the Mechanism of Surface Boiling at Atmospheric Pressure.

B. Authors: Parker Olin Chapman

Norman Fred Geer

C. Submitted for the Degree of Naval Engineer in the Department of Naval Architecture and Marine Engineering on 18 May, 1951.

D. The object of this thesis is to experimentally obtain heat transfer data for subcooled water flowing vertically upward over a heated flat plate at atmospheric pressure, to photograph the bubble formation during surface boiling and to relate the bubble size, population and trajectory with the variables of surface temperature, liquid subcooling and flow rate.

The results in the form of plots and photographs show that a pronounced increase in the heat flux density occurs under conditions of surface boiling, that there is a transition zone between non-boiling and fully developed boiling in which eddy turbulence has an effect on the heat transfer rate and that photographic speeds greater than two micro-seconds are required to completely stop the action of vapor bubble formation. Over the range of variables studied it was found that vapor bubble velocities are of the order of 1000 ft/sec., that velocity is normal to the heated surface and that bubble population is not a

cyclical phenomenon. The effect of the presence of bubbles in decreasing the density of the bulk water was observed to be very slight, order of magnitude was one percent.

The results of this investigation seem to lend support to the hypothesis postulated by Rohsenow and Clark that the pronounced increase in heat transfer rate coinciding with surface boiling in forced convection is due primarily to the agitation of the quiescent layers of liquid adjacent to the heated surface resulting from the motion of vapor bubbles being generated there.

Cambridge, Massachusetts
May 18, 1951

Professor J. S. Newell
Secretary of the Faculty
Massachusetts Institute of Technology
Cambridge, Massachusetts

Dear Sir:

In accordance with the requirements for the degree of Naval Engineer, we submit herewith a thesis entitled "A Photographic Study of the Mechanism of Surface Boiling at Atmospheric Pressure."

Respectfully submitted,

ACKNOWLEDGEMENTS

The authors wish to express their appreciation to Professor Warren M. Rohsenow for suggesting the nature of the investigation and for his aid in interpretation of the results.

Our sincere thanks are due Mr. John A. Clark for guidance and advice throughout the entire investigation.

The cooperation and assistance of Mr. Fred Johnson in assembling the test equipment was greatly appreciated.

TABLE OF CONTENTS

LIST OF FIGURES

LIST OF FIGURES (Continued)

I. INTRODUCTION

Heat transfer at high density of heat flux has become increasingly important in recent years due to the many scientific and industrial applications requiring extremely high rates of heat transfer per unit area. The mechanism of heat transfer at high flux density to water is of particular interest and importance. Whereas, the properties of water are well established and much is known about heat transfer to water in the non-boiling region, there has been a scarcity of substantiated data in the "local" or "surface boiling" region.

"Surface boiling" is a form of nucleate boiling occurring when a subcooled liquid is brought into contact with a heated surface, hot enough to generate vapor at the surface of the heater. The vapor bubbles formed subsequently condense in the colder liquid.

Earlier investigations in this field (9), (10) established that the important variables to be considered in a study of surface boiling were velocity, pressure, bulk temperature, concentration of dissolved gas in the fluid, size of the heat transfer surface and the nature of the surface. All of the earlier work has shown that the heat transfer rate increases sharply in the region of surface boiling, but the data thus far has not yielded adequately to correlation by any means so that no generalized equations exist for predicting heat transfer coefficients or the

maximum heat flux density that may be realized. Because the increase in heat flux density occurs when vapor bubbles form there is probably some correlation between the two, since other conditions remain essentially the same. For this reason photographic study of the mechanism of bubble formation is indicated. McAdams et al (8) have taken high speed motion pictures of the boiling process associated with forced convection. These pictures and attendant data have been analyzed by Rohsenow and Clark (5) who have demonstrated that the energy required to form all the visible bubbles is a very small fraction of the increased heat transfer in the surface boiling region. They have postulated that the high rate of heat transfer associated with surface boiling in a sub-cooled liquid is due primarily to the violent agitation of the quiescent layers of liquid adjacent to the heated surface resulting from the motion of vapor bubbles being generated there.

It is the purpose of this thesis to employ various experimental techniques to photograph the bubble formation during forced convection over a vertical heated plate. It is hoped that data and pictures thus obtained may yield some correlation between bubble population and size with other variables such as sub-cooling and fluid velocity. Further, it is hoped that necessary modifications or changes in techniques of bubble photography will result from this investigation in order that such changes may be utilized in a later, more detailed study at high pressures.

II. Procedure

Basically, the procedure followed was to obtain, experimentally, values of heat flux density and the corredponding temperature difference for distilled water flowing vertically upward through a rectangular test section, the back wall of which was a heated flat plate. The variables of velocity and bulk temperature were independently controlled and pressure at the heated strip was maintained at one atmosphere. A series of high speed photographs and high speed motion pictures were taken to show the variation in bubble population and size under the various conditions.

III. Results

The results of this investigation are summarized in figures XVI to XXVIII. The results of the high speed motion pictures have not been fully analyzed to date. All film is in the possession of Mr. John A. Clark, Mechanical Engineering Department, M.I.T. The film reels are numbered corresponding to the numbering as shown in the original data, Appendix I.

IV. DISCUSSION OF RESULTS

The results of the experimental runs are plotted in figures XVIII through XXII as heat flux density, Q/A, versus the temperature difference, $t_w - t_b$. In the non-boiling region the normal linear relationship exists between Q/A and Δt. As local boiling commences a pronounced increase in the slope of the curve occurs. At conditions of high surface boiling this approximates a linear relationship whose slope is considerably higher than that in the non-boiling region. The increase in slope in the transition zone between non-boiling and boiling occurs at lower values of Δt and is gentler than that observed by earlier investigators (5), (7), (8). This is accounted for by the fact that the liquid during testing was only partially degassed. The heated strip, acting as a degasser, caused air bubbles to form before the water vapor bubbles would normally appear. McAdams et al (8) have shown that with gasified water the heat transfer rate begins to increase before the boiling temperature of the water is reached. Their experimental results are replotted here as fig. XXV. The effect of dissolved gas becomes decreasingly important as the boiling rate increases.

The fact that gasified water shows an increase in heat flux density before degasified water lends support to the hypothesis of Rohsenow and Clarke (5) who have

postulated that it is the agitation of the quiescent layer next to the heater strip which permits the pronounced increase in heat transfer rate. Gas bubbles could theoretically cause this as well as water vapor bubbles.

A more striking support of this hypothesis is seen from examination of fig. XVII which is the plot showing correlation of data in the boiling region. Between non-boiling and fully developed boiling there exists a transition region in which we have in addition to eddy turbulence, turbulence as a result of bubble motion, which for the purpose of description we will call bubble turbulence. The effects of bubble turbulence and eddy turbulence are presumably of the same order of magnitude at first but as the surface becomes more heated the bubble action becomes more vigorous resulting in bubble turbulence becoming of a higher order of magnitude. This effect becomes more pronounced with increased heating, resulting in a negligible velocity effect at fully developed boiling.

Figure XXVIII is a composite photograph showing bubble formation at velocities of 5 ft/sec. and 1.7 ft/sec. The condition at the lower velocity run is relatively closer to the region in which fluid velocity does not affect the heat transfer rate. In the higher velocity run the bubble agitation is less vigorous yet the Q/A is larger indicating that the eddy turbulence is influencing the heat transfer considerably.

Fig. XXI is a composite of figures XVIII, XIX and XX showing the effect of velocity to be a higher Q/A value reached before surface boiling commences.

Fig. XXII is a plot of Q/A versus $\Delta t = t_w - t_b$ at 1 ft/sec. showing the effect of a change in subcooling. Since all our runs were at atmospheric pressure this is merely a change in bulk temperature. It is seen that incipient boiling occurs at a lower value of Q/A as bulk water temperature is increased.

Fig. XXVII is a composite photograph of 16 runs at the same velocity showing the variation of bubble size and population with subcooling and heat flux density, Q/A. These pictures were taken at an estimated speed of two micro-seconds and show that the action of bubble formation is still not fully stopped. Measurement of the bubble blur indicates a bubble velocity in the order of 1000 ft/sec. This velocity appears normal to the heating surface. The large amount of small dots that are visible out in the stream are apparently bubbles of non-condensable gas which have been liberated at the heater strip. The number and penetration of these bubbles far exceeds the number and penetration of water vapor bubbles. In no case is a water vapor bubble seen to penetrate more than 0.05". Gas bubbles persist through the visible length of the test section above the heater strip and the number is so great at high flux densities that they appear as a white froth. The speed of these bubbles as they leave

the wall is relatively slow compared with the speed of water vapor bubbles. They appear in sharp focus at 2 micro-seconds but are blurred at 2×10^{-3} seconds. (See picture No.4, figure XVIII.) A plot of gas bubble trajectory was attempted but discarded as inconclusive since it was impossible to tell whether the gas bubble commenced its penetration from the surface of the heater strip or from the colder area adjacent to the heater strip.

Fig. XXIII shows the results of an estimated density change of the water next to the heater strip. The volume investigated was near the middle length of the strip at a distance into the stream of .045". This dimension was taken to approximate the hydraulic radius of a tubular heating element used in a high pressure study (4). Small sections of the films in figure XXVI were enlarged to the limit of definition, about 21 x. The bubbles in evidence were counted and diameters measured. The results are tabulated as table V . The root mean cube diameter was calculated and the percentage of volume occupied by the bubbles determined for two different assumed conditions. The first assumption was that the bubbles seen and counted were only those for a width across the heater strip of one bubble diameter, i.e., each bubble theoretically could be blocking the view of a row of bubbles. The second assumption was that the bubbles seen and counted were all of the bubbles existing for the full width of the heater strip. From observation of these and many other runs the authors

believe the second assumption to be much the better of the two. The results of both assumptions are plotted in fig. XXIII as percent change in volume against heat flux density for three different subcoolings. It is seen that the lower subcooling, i.e., the warmer bulk water results in the greatest density change but this is slight, in the order of one percent. It might be expected that a much larger decrease in density would appear at or approaching burnout. Information in this region is to be desired.

The high speed motion picture study is as yet incomplete but it was found that an estimated speed of 3000 frames per second is not fast enough to show the formation and growth of the bubbles. Approximately 1/3 of the bubbles can be seen in 2 consecutive frames. The remainder apparently condense between frames. In no case did the same bubble appear in more than 3 adjacent frames. It will be necessary to use much higher frame speeds to plot bubble trajectory. Reel #4 taken at $Q/A = 282{,}000$, 90° subcooling and fluid velocity = 1.7 ft/sec. proved to be the best reel for analysis. The estimated effective exposure time for this reel was 1/15,000 sec. per frameand bubble action was not fully stopped. A bubble count of 52 consecutive frames was made using a micro-film viewer and when plotted against frame number a random scatter with no definite cycle in evidence was obtained. This plot appears as fig. XXV.

Thus, with this meager data, it appears that with no pronounced cycling of bubble population, density data can be obtained from still pictures. However, if other information is desired such as bubble trajectory it is obvious that still photography will be inadequate. It was apparent from examination of the film that the camera speed at the end of the reel was higher than at the first part. It will be necessary in any future motion picture study to operate a timing light in conjunction with the camera for accurate speed measurement.

V. Conclusion

1. Agitation of the quiescent layer adjacent to the flat plate heater strip by bubble action apparently is primarily responsible for the increased heat flux density under conditions of surface boiling.
2. A well defined and reproduceable transition zone exists between non-boiling and fully developed boiling. The agitation responsible for this is due to eddy turbulence and bubble turbulence.
3. After passing through the transition zone into fully developed surface boiling, the effect of velocity is negligible.
4. To get a single vapor bubble to persist for as much as ten (10) frames, motion picture speeds in the order of 15-20,000 frames per second are indicated.
5. The penetration of non-condensable vapor bubbles is much greater than that of the water vapor bubbles.
6. The speed of the water vapor bubbles leaving the wall is of the order of 1000 ft/sec. The speed of the non-condensable vapor bubbles is much less.
7. There appears to be no evidence of a cyclical change in bubble population at a subcooling of 90°F.
8. The bubble formation during surface boiling decreases the density very slightly, the order of magnitude being one percent.

VI. RECOMMENDATIONS

1. When visual studies involve a flat heating surface, the surface should be maintained as narrow as possible. This will prevent hidding bubbles and also aid in having all bubbles in focus when photographed.
2. A preheater should be installed to maintain the sub-cooling temperature. It should have enough capacity to heat the water from about 60°F to the saturation temperature. The cooler could then be used to cool the water leaving the test section to prevent pump cavitation.
3. Small pipe diameter should be avoided as much as possible to reduce pressure losses in the circuit.
4. In using rectangular test sections the entrance for the water should be as smooth as possible to avoid cavitation at high velocities.
5. For better control of test conditions special care should be taken in designing the test section to insure that it is air tight. The use of lucite or other plastic materials is not recommended because of their lack of rigidity.
6. Better means of shielding the outer wall thermocouples should be devised. A successful method might be to use a dead air space with a heater consisting of an electrically heated strip parallel to the test section heater strip.

7. Higher speed motion pictures should be obtained in order to definitely establish whether or not cycling exists. If it does not exist high speed still pictures would be sufficient for visual studies.
8. The effect of bubble formation on bulk density should be investigated at and near burnout conditions.
9. Further visual study should be made to investigate the effect of mechanical agitation of the quiescent layer near the heater strip.

APPENDIX A

NOMENCLATURE

A	Area, sq. in.
b	Heater strip width, in.
^{o}C	Degrees, Centigrade scale
C	Coefficient of discharge, dimension less
C_p	Specific heat, BTU/lb.-^{o}F
D	Diameter, ft.
d_m	Root mean cube bubble diameter, in.
E	Voltage, volts
^{o}F	Degrees, Fahrenheit scale
G	Conversion factor, 3.413×10^{3} BTU/K.W.-Hr.
g	32.2 ft/sec. - sec.
H	Head, ft. of fluid
h	Heat transfer coefficient, BTU/hr-sq.ft.-^{o}F
I	Current, amperes
J	$\left(Nu/Pr^{\frac{1}{3}} Re\right) x \left(\frac{\nu_w}{\nu_b}\right)^{0.14}$, dimensionless
K	Flow coefficient, dimensionless
k	Thermal conductivity, BTU/hr.-sq.ft. $\frac{^{o}F}{ft}$
L	Length, ft.
l	Length of heater strip used in bubble count, in.
m	$G \left(\frac{dE}{dx}\right)^{2} \Big/ 2 \rho_o k_o$) ^{o}F/sq.in.
N_{PR}	Prandtl number, dimensionless
N_{RE}	Reynolds number, dimensionless

N_u	Nusselt number, dimensionless
p	Pressure, lbs./sq.in.
Q	BTU/hr.
Q/A	Heat flux density, BTU/hr.sq.ft.
R_d	Reynolds number based on orifice diameter, dimensionless
r_h	Hydraulic radius, in.
r_1	$\frac{v_c - v_b}{v_c}$, dimensionless
r_2	$\frac{v_d - v_b}{v_d}$, dimensionless
t_a	air temperature, ^oF
t_b	Liquid bulk temperature, ^oF
t_m	Mean temperature through heater element, ^oF
t_o	Temperature of heater element, outside wall, ^oF
t_w	Temperature of heater element, inside wall, ^oF
t_{sat}	Superheat, ^oF
V	Mean stream velocity, ft/sec.
v_b	Volume of bubbles, cu.in.
v_c	Volume of water with no bubbles, one bubble diameter wide, cu.in.
v_d	Volume of water with no bubbles, 1/2" wide, cu.in.
w	Mass rate of flow, lbs./sec.
x	Distance along heater strip, in.
y	Heater strip thickness, in.
α	Temperature coefficient of electrical resistivity

β	Temperature coefficient of thermal conductivity
Δ	Difference
ρ	Density, lbs./cu.ft.
ρ	Electrical resistivity, ohm-in.
μ_b	Viscosity based on bulk temperature, lbs/hr.ft.
μ_w	Viscosity based on wall temperature, lbs/hr-ft.

APPENDIX B

Orifice Calculations for Design

Max. vel in test section = 30 ft/sec.

Cross-sect. area test section = .00455 R^2 = .655 in.^{2}

D_i of 1" Cu tube (type "L") = 1.025"

Cross-sect. area of tube = .825 in.^{2} = .00573 ft.^{2}

Max. vel. in tube = $\frac{655}{825}$ x 30 = 23.8 ft/sec.

At max. flow rate of 23.8 ft/sec. in tube, at 112°F,

w = 62x23.8x.00573 = 8.45 ~~#~~/sec.

Flow equation: $w = \dfrac{CA_2\sqrt{2\rho g \Delta p}}{12\sqrt{1-\left(\frac{A_2}{A_1}\right)^2}}$

Let max. ht. of Hg. in manometer = 45"

then: Δp = inches Hg. under water x .4534

(.4534 is factor for 70" water)

$\Delta p = 45\ (.4534) = 20.4$

$$w \times 12\sqrt{1-\left(\frac{A_2}{A_1}\right)^2} = CA_2\sqrt{2\rho g \Delta p}$$

$$144\ w^2\left(1-\left(\frac{A_2}{A_1}\right)^2\right) = C^2A_2^2(2\rho g \Delta p)$$

$$1 - \frac{A_2^2}{A_1^2} \Big/ A_2 = \frac{C^2(2\rho g \Delta p)}{144\ w^2}$$

Assume $C = .6$: $\frac{1}{A_2^2} - \frac{1}{A_1^2} = \frac{C^2(2\rho g \Delta p)}{144\, w^2}$

$$\frac{1}{A_2^2} - \frac{1}{.680} = \frac{.36(2x62x32.2x20.4)}{144x71.3}$$

$$\frac{1}{A_2^2} - 1.47 = 2.855$$

$$\frac{1}{A_2^2} = 4.325;\quad A_2^2 = .231;\quad A_2 = \underline{\underline{.481 \text{ in.}^2}}$$

$$\frac{A_2}{A_1} = \frac{.481}{.825} = .583 = \frac{D_2^2}{D_1^2}$$

$$\frac{D_2}{D_1} = .765;\qquad \underline{\underline{D_2 = .784"}}$$

$$R_d = \frac{48w}{\pi D\mu} = \frac{48x8.45}{\pi\, x.784x43x10^{-5}} = 3.82x10^5$$

for min. ht. Hg = 4"

then $\Delta p = 4x.4534 = 1.815$ psi

$\sqrt{\Delta p} = 1.347$, $\left(\frac{A_2}{A_1}\right)^2 = (.583)^2 = .339$

$$w = \frac{CA_2\sqrt{2\rho g \Delta p}}{12\sqrt{1-\left(\frac{A_2}{A_1}\right)^2}}$$

$$w = \frac{.6x.481}{12x.814}\sqrt{2x62x32.2}$$

$\underline{\underline{w = 2.51 \text{ \#/sec.}}}$

$w = \rho AV$

$2.51 = 6\ 2x.00455xV$

$V = 8.91$ ft/sec. in test section

$R_d = \frac{2.51}{8.45} x3.82x10^5 = 1.134x10^5$

for orifice (B)

max. ht. Hg = 45 " = Δp = 20.4 psi

$$\frac{1}{A_2^2} - 1.47 = 2.855 \times \frac{71.3}{6.3} = 32.25$$

$$\sqrt{\frac{1}{A_2^2}} = \sqrt{33.72} = 6.1$$

$$A_2 = .164 \text{ in.}^2$$

$$\frac{A_2}{A_1} = \frac{.164}{.825} = .199 = \frac{D_2^2}{D_1^2}$$

$$\frac{D_2}{D_1} = .446$$

$$D_2 = .457"$$

At min. flow of 1 '/sec thru T.S.: w = .282 #/sec.

$$.282 = \frac{.6(.164)}{12\sqrt{1-.0395}} \sqrt{62x2x32.2}\ \sqrt{\Delta p}$$

$$.282 = \frac{.6(.164)}{(12)(.98)} x63.2\ \sqrt{\Delta p}$$

$$\sqrt{\Delta p} = \frac{.282x20(.09)}{.164x63.2} = .533$$

$$\Delta p = .284 \text{ psi}$$

$$\frac{.284}{.4534} = .628"$$

.628x2.54=1.59 cm. = 15.9 mm Hg.

Since this is such a small reading on the manometer we will manufacture a third orifice of approximately .300" diameter to handle low flow rates.

As manufactured the dimensions of our three orifice plates are as follows:

orifice "A" - dia. = .781"

"B" - " = .465"

"C" - " = .303"

$$w = \frac{K\, A_{ORI} \sqrt{2g\rho\Delta p}}{12} \qquad \text{where K = FLOW COEF.}$$

$$K = \frac{12 \times w}{A_{ORI} \sqrt{2g\rho}\sqrt{\Delta p}}$$

$$K = \frac{48}{\pi D_{ORI}^2 \sqrt{2 \times 32.2 \times 62.33}} \sqrt{\frac{.4535}{2.54}} \times \frac{w}{\sqrt{\Delta H}}$$

$$R_d = \frac{48\, w}{\pi D \mu} = \frac{48\, w}{\pi D\, .705 \times 10^{-3}}$$

ORIFICE	K	RE
"A"	$.937 \frac{w}{\sqrt{\Delta H}}$	$2.775 \times 10^4 \times w$
"B"	2.64 "	$4.67 \times 10^4 \times w$
"C"	6.21 "	$7.15 \times 10^4 \times w$

DATA FOR ORIFICE CALIBRATION

ORIFICE "A" - DIA. = .781

30 Jan.1951

Water Temp.: 65°F CM. of HG Right Tube	Left Tube	Sum	Lbs. Flow	Secs Time	Mass Rate W	$W/\sqrt{\Delta H}$	Calculated Values K	R_d
51.8	43.8	95.6	300	38	7.9	.807	.756	2.19×10^5
5.9	43.9	95.8	300	37.5	8.0	.817	.765	2.22×10^5
47.6	40.5	88.1	300	40	7.5	.798	.748	2.08×10^5
47.5	40.4	87.9	300	40	7.5	.800	.749	2.08×10^5
44.3	38.0	82.3	300	41	7.32	.806	.755	2.03×10^5
40.8	35.0	75.8	300	42	7.15	.82	.768	1.982×10^5
37.2	31.9	69.1	300	44	6.82	.82	.768	1.892×10^5
34.5	29.8	64.3	300	46	6.52	.812	.761	1.81×10^5
32.1	27.7	59.8	300	48	6.25	.808	.757	1.734×10^5
29.6	25.6	55.2	300	49	6.12	.822	.770	1.70×10^5
26.5	23.0	49.5	300	52	5.77	.819	.767	1.60×10^5
23.1	20.1	43.2	300	55.5	5.41	.822	.770	1.50×10^5
19.9	17.3	37.2	300	60	5.00	.818	.766	1.387×10^5
16.7	14.5	31.2	300	66	4.55	.813	.762	1.262×10^5
12.5	11.0	23.5	300	75	4.00	.825	.773	1.11×10^5
10.3	9.1	19.4	300	83	3.62	.821	.769	1.005×10^5
9	7.9	16.9	300	88.5	3.39	.824	.772	9.41×10^4
7.8	6.9	14.7	300	95	3.16	.822	.770	8.77×10^4
5.8	5.1	10.9	300	109	2.75	.832	.780	7.63×10^4
4.1	3.7	7.8	300	128	2.34	.839	.786	6.50×10^4
2.8	2.6	5.4	300	155	1.935	.832	.780	5.37×10^4

TABLE I

DATA FOR ORIFICE CALIBRATION

ORIFICE "B" - DIA. = .465

30 Jan. 1941

Water Temp.: 65°

CM. of HG Right Tube	CM. of HG Left Tube	Sum	Lbs. Flow	Secs. Time	Mass Rate W	Calculated Values $W/\sqrt{\Delta H}$	K	R_d
70	51.4	121.4	100	40	2.5	.227	.600	1.168×10^5
65.6	48.3	113.9	100	41.5	2.41	.226	.597	1.125×10^5
59.3	44.0	103.3	100	43.5	2.3	.226	.597	1.075×10^5
56.1	41.8	97.9	100	45	2.22	.224	.592	1.036×10^5
52.3	39.2	91.5	100	46.5	2.15	.224	.592	1.005×10^5
47.4	35.6	83.0	100	48	2.08	.228	.602	9.71×10^4
41.6	31.6	73.2	100	51	1.96	.229	.605	9.15×10^4
34.5	26.5	61.0	100	56.5	1.77	.226	.597	8.26×10^4
25.8	20.0	45.8	100	64.5	1.55	.229	.605	7.23×10^4
18.7	14.7	33.4	100	75.5	1.325	.229	.605	6.18×10^4
14.1	11.1	25.2	100	88	1.135	.226	.597	5.30×10^4
10.5	8.4	18.9	50	51	.98	.225	.594	4.575×10^4
8.7	6.9	15.6	50	55	.909	.230	.607	4.24×10^4
4.7	3.7	8.4	50	77	.65	.224	.592	3.03×10^4
3.8	2.9	6.7	50	85	.588	.227	.600	2.745×10^4

TABLE II.

DATA FOR ORIFICE CALIBRATION

ORIFICE "C" - DIA. = .303"

31 Jan. 1951

Water Temp.: 65°F

CM. of HG Right Tube	CM. of HG Left Tube	Sum	Lbs. Flow	Secs. Time	Mass Rate W	Calculated Values $W/\sqrt{\Delta H}$	K	R_d
70.1	45.1	115.2	50	48	1.042	.1098	.681	7.45×10^4
61.3	40.0	101.3	50	51.5	.971	.0965	.598	6.94×10^4
55.7	36.8	92.5	50	55	.91	.0945	.586	6.51×10^4
49	32.6	81.6	50	58	.863	.0954	.592	6.17×10^4
43.2	29.2	72.4	50	61.5	.813	.0954	.592	5.82×10^4
37.4	26.1	63.5	50	65	.77	.0964	.598	5.51×10^4
31.2	21.4	52.6	50	72	.695	.0956	.593	4.97×10^4
24.3	16.9	41.2	50	80	.625	.0972	.603	4.47×10^4
18.9	13.1	32.0	50	91.5	.547	.0965	.598	3.91×10^4
15	10.4	25.4	50	102.5	.488	.0965	.598	3.49×10^4
11.1	7.7	18.8	50	119	.420	.0967	.600	3.00×10^4
8.7	6.0	14.7	50	134	.373	.0973	.604	2.67×10^4
6.2	4.2	10.4	50	150	.333	.103	.640	2.38×10^4
4.4	2.9	7.3	50	192	.261	.0963	.597	1.865×10^4
2.4	1.5	3.9	50	271	.1845	.0933	.578	1.32×10^4
2.9	2.0	4.9	50	241	.208	.0940	.583	1.49×10^4
3.7	2.5	6.2	50	206	.243	.0973	.604	1.74×10^4
5.15	3.6	8.75	50	174	.288	.0971	.602	2.06×10^4
7.4	5.3	12.7	50	144	.347	.0973	.604	2.48×10^4

TABLE III

Appendix C

Thermocouple Calibration

16 Feb. 1951

Room temperature = 24°C

Barometer = 783.3 mm Hg.

Correction for temp = - 3.07 mm Hg

Corrected baro. = 780.2 mm Hg.

Cold junction = ice and water

Hot junction = Napthalene vapor

Boiling point correction formula:

$$t_p = 217.96 + .207\,(t_p+273.1)\log_{10}\left(\frac{P}{760}\right)$$

Potentiometer reading = $\frac{20.58}{2}$ m.v. = 10.29 m.v. = $E_{OBS.}$

$$t_p\ ^{\circ}C = 217.96+.207\,(t_p+273.1)\log_{10}\left(\frac{780.2}{760}\right)$$

$$= 217.96+.00238\,(t_p + 273.1)$$

$$t_p{}^{\circ}C = 219.13$$

at 219.13°C, E_{STD} = 10.312 m.v.

$$\Delta E = E_{OBS} - E_{STD} = 10.29-10.312 = -.022 \text{ m.v.}$$

Second run using steam for hot point

Boiling point correction formula:

$$t_p{}^{\circ}C = 100.000+.03686\,(p-760)-.0000202\,(p-760)^2$$

Potentiometer reading = $\frac{8.6}{2}$ m.v. = 4.3 m.v. = $E_{OBS.}$

$$t_p{}^{\circ}C = 100.000+.03686(780.2-760)-.0000202(78.02-760)^2$$

$$t_p{}^{\circ}C = 100.737$$

at t_p°C = 100.737, E_{STD} = 4.3105 m.v.

$E = E_{OBS} - E_{STD} = 4.300 - 4.3105 = -.0105$ m.v.

APPENDIX D

DETAILS OF PROCEDURE

Filling System and Starting Pump

The system was filled from the supply used in the high pressure study. Distilled water was used and the water was heated to boiling to reduce the concentration of dissolved air. All control valves and the air vent were open. A rubber tube was connected to the vent and the end of the tube was placed in a distilled water bottle which contained water at a level above the test section. This connection was made for the purpose of eliminating low pressures at the test section when the pump was started. (The authors were unable to make the test section air tight and at low pressures air leaked in along the downstream, i.e., upper, edge of the heater strip.)

After filling the system the filling valve (not shown in fig. VII) and the flow control valve were closed. The top of the pressure vessel was opened to the atmosphere thereby assuring atmospheric pressure plus about five feet of water pressure at the suction of the pump. When the pump was not running the pressure at the system vent was also controlling the pressure at the pump, with the water in the pressure vessel and the water in the bottle seeking a common level if given enough time. The pump was then started and after it was running the filling vent was closed leaving the pressure vessel in control of the system pressure. The reason for leaving the vent open during

starting was to prevent a momentary low pressure at the test section, drawing in air around the heater strip. The small tube leading from the pressure vessel prevented this vessel alone from controlling the sudden change in pressure.

After the pump was started the top of the pressure vessel was shut off from the atmosphere and connected to a city water operated, venturi aspirator. The aspirator was used to lower the air pressure in the pressure vessel, thereby lowering the pressure on the system. The pressure was lowered until the first signs of air leaking into the test section were detected. This indicated about atmospheric pressure at the heater strip. (In reality it was very slightly above atmospheric because of a small amount of air pressure in back of the strip due to shielding air.)

The flow control valve was then opened and the pressure in the pressure vessel adjusted to obtain atmospheric pressure at the test section. It was originally planned to use a manometer to tell when atmospheric pressure at the test section was reached. The manometer was not connected directly to the test section but between the vent valve and the system. The manometer was then calibrated against the flow velocity by noting its reading when air first leaked into the system. Had the air leak been absent it would have been necessary to connect the manometer directly to the test section. As it turned out

later the leak increased to such an extent that it was necessary to maintain a steady and pronounced leakage of air in order to keep the thermocouples in back of the strip dry. Then the pressure manometer served only as a guide to the system pressure.

Deaeration

When first operating the equipment considerable difficulty was experienced in removing air from the system. In order to remove the small air bubbles entering the system through the above mentioned leak the deaerator was designed (as shown in fig. X). The water entered the three inch inner pipe tangentially to induce a swirl in the water and force the air bubbles toward the center and upward. Because of the large diameters involved in comparison to the one inch pipe the velocities were reduced to permit the air to rise to the top of the deaerator. The deaerator was connected near the suction side of the pump, in the low pressure part of the system, which increased the size of the bubbles. Air was removed periodically from the deaerator by use of the aspirator. This method of air removal was very satisfactory to velocities up to about 7 or 8 ft/sec through the test section. At higher velocities it could not remove the air as fast as it was drawn into the system.

The water used for all runs was distilled water obtained from Belmont Spring Water Company. As received this water showed an O_2 concentration of 5-6 m.l. per liter. Boiling before filling reduced this concentration

to the order of 1-1.5 m.l. per liter. Samples taken during runs indicated a dissolved oxygen concentration of approximately 3.2 m.l./per liter showing that some of the leakage air went into solution. This figure remained essentially constant throughout the runs. O_2 determination was made using the Winkler method.

Observed Data

For calculating results the following data was obtained: temperature of incoming and exit water, temperature in the center of the back of the heater strip, shielding air temperature, volts, amperes and pressure drop across the orifice.

The temperature rise of the water through the test section was so small that it could not be detected in the majority of runs. When the exit temperature did vary considerable uncertainty existed as to whether a temperature equilibrium had been established in the water. The bulk temperature used in calculations was the temperature of the incoming water.

Because the only heat added to the water was in the test section, the highest bulk temperature that could be held for all velocities and heat flux densities was about 122°F. Higher bulk temperatures could be maintained at high flux densities and some isolated data was obtained in this region.

In order to get the true temperature of the back of the heater strip the temperature of the shielding air was

adjusted until the air temperature thermocouple read the same as the heater strip thermocouple. It was found that this temperature balance was very critical. One tenth milli-volt difference (about 2°F.) between the air thermocouple and the heater strip thermocouple would mean a difference of 10°F. from the true heater strip temperature.

Photographic Technique

Photographic technique was developed by William B. Whiston and the techniques employed, with varying measures of success, are fully described by him in (6). Only the more successful will be described here.

Still pictures

Camera used was a 4x5 Speed Graphic. First pictures were flood lighted with 1/1000 sec. shutter speed. This did not stop the action so for the next runs Edgerton type speed lights were used at successive speeds of 1/2500 sec., 1/10,000 sec and 2 micro-seconds. The highest speed was required to effectively stop all action.

High Speed Motion Pictures

Camera used was Eastman type III High Speed 16 m.m. motion picture camera, operated at 3,000 frames per second which gave individual exposure time of 1/15,00 sec.

SET-UP OF APPARATUS

(a) Flow Circuit

A schematic diagram of the flow circuit appears in fig. VII. The pressure vessel, filling chamber, ion-exchanger, pump and associated piping and valves were located within a test cell. These units were designed and used for other phases of bubble study, (3) and (4), and were made available to us all assembled. The part of the system external to the test cell was constructed by the authors. A photograph of this appears as fig. VIII. Circuit piping and fittings were of commercial 1" copper sweated with soft solder except at throttle valve and heat exchanger ends where silver braze was used.

Pressure drop across the calibrated orifices used in flow measurement was measured on a mercury "U" tube manometer constructed by the authors.

Copper to copper unions were used to connect the flow circuit external to the test cell with the internal leads which were brought out through holes drilled in the wall of the test cell. Unions were also used to connect the test section into the flow circuit and the orifice section into the flow circuit.

(b). Test Section

The test section is the heart of the apparatus and the component about which the rest of the circuit was designed and constructed. The test section employed was designed and constructed by Mr. Eugene E. Drucker (2)

for the specific purpose for which it was employed. Design calcultions and detailed drawings appear in (2) and a brief description of the test section will suffice here. The test section is rectangular constructed of a transparent plastic called "Boilable Lucite". The internal cross-sectional area is 7/8"x3/4", and wall thickness is 1/4". The front and back walls of the test section are flanged and the side walls are grooved to receive these flanges with a thin rubber tube between to act as a gasket. The end connection are made by cementing blocks of lucite to the four sides at each end and drilling them to receive 1/4" Allen set screws which are screwed into a brass plate at each end, 3" square 1" thick. Thin sheet rubber is used as a gasket at each end. The brass end plates are drilled to receive 3/4" extra strong brass pipe, 3" long. The inside diameter of this brass pipe is tapered starting with nominal dimensions at 1" from the end and increasing the inside diameter to the inside diameter of 1" copper tubing. The external diameter is turned down, starting 1" from the end to the inside diameter of 1" copper tubing. This enables the 1" copper tubing to fit over the brass pipe for a distance of 1" and permits a smooth reduction in cross-sectional area for the flow entering the test section and expansion when leaving. The back wall of the test section is cut out for a distance of 6" commencing at 2" from the exit end. The overall length of the

lucite walls is 17". The heater element is inserted in this cut-out section and consists of a stainless steel strip, 1/2" wide, 4" long and .0193" thick. This strip is cemented in a laminated asbestos fabric phenolic resin called "AA-39", manufactured by the Formica Company of Cincinnati, Ohio. The bonding material used is "Bostick" cement No. 7026, manufactured by the B.B. Chemical Company of Cambridge, Massachusetts. The entire "formica" section is fitted into and flush with the cut-out section of lucite by built up blocks of plastic, drilled and bolted to the "formica", which is tapped for Allen set screws.

Copper bus bars are silver brazed to the back ends of the heater strip for power leads, lead out through the "formica". Three thermocouple junctions are cemented on to the back of the heater strip with an insulating layer of Bostik cement. The sides of the "formica" (block) are cut out to provide a small space in back of the heater strip to lead out the thermocouple wires and to permit a space for heated air to be introduced to shield the thermocouples. A fourth thermocouple is located in this space to measure heated air temperature.

Considerable difficulty was encountered in assembling the test section. The methods originally designed to seal against leakage proved inadequate. It was finally necessary to drill and tap the edges of the lucite walls and bolt the sections tightly together and

in addition to seal all external seams with Bostik cement. The latter was undertaken as a least resort since the original intention was to join the test section so that it could be readily disassembled for replacement of heater strip if necessary.

(c). Heat Exchanger

The heat exchanger was built in accordance with reference (2) and is simply a tube-in tube exchanger with the main circuit piping continuous inside a 6' length of 1 1/4" standard iron pipe. City water is the cooling medium and is controlled by valves at entrance and exit.

(d). Pump

The pump providing the flow was a Westinghouse totally enclosed centrifugal pump, model 30A, 220 volts, 3 phase, 60 cycle; operating characteristics and a description of this pump appears in (4).

(e). Orifices

The orifices were designed and constructed by the authors; detailed calculations appear in Appendix B and are discussed under "Flow Measurements", section . Fig. IX is a drawing of the orifice section.

(f) Deaerator

Sketch of the deaerator appears as fig. X.

(g) Power Supply

Power for the heater strip was furnished by a motor-

generator set, the name plate data for which appears below.

D.C. Generator

General Electric Co.
Model No.53A532
Serial No.1897572
KW - 15
Volts - 15
Amps - 1000
RMP - 1200
Separately excited

A.C. Driving Motor

Westinghouse Electric Co.
Type-CS
Serial No.10179
Phase - 3
Cycles - 60
Volts - 220
Amps - 65

(h) Potentiometer

The potentiometer used for temperature and power measurements was manufactured by the Rubicon Company of Philadelphia, Pennsylvania, Serial #51176, Model #2703.

AIR HEATER

To eliminate heat loss from the heater strip other than to the system water and to insulate the back side of the heater strip bearing the thermocouples, heated air was introducted into the space provided. To provide the air flow, a line was run from the low pressure air system located on the test floor. This was reduced to a 1/4" copper tube with a globe valve installed for control. A simple heater with more than sufficient capacity was constructed as follows: a two foot length of 3/8" stainless steel tubing was filled with stainless

steel wool and secured to 1/4" copper tubing at inlet and outlet by two inch ceramic insulating sleeves. The jointing compound used was "Sauereisen" porcelain cement. A thirty to one step-down auto-transformer with input controlled by a Variac connected to city 110 v. lighting circuit provided the current necessary to heat the tube and hence the air passing through it. Leads from the transformer were clamped directly to the stainless steel tube, a distance of 16 1/2 inches apart. Dimensions of tube and separation of power leads was obtained from reference (3) which indicated these details of construction for a 1000 watt heater. Sketch of air heater appears as fig. XI.

INSTRUMENTATION

1. Flow Measurement

Water velocities were measured by means of calibrated orifices. Three different sizes being used to cover the desired range without undesirably high manometer readings. The orifices were constructed by stainless steel, 1/8" thick and were designed, in so far as possible, according to procedure outlined in A.S.M.E. Power Test Codes, 1940, Part 5, Chapter 4. Slight departure from recommendations in above reference was necessitated by the range of pressure drop to be covered. Design calculations appear in Appendix B.

After manufacture, orifices were calibrated over the desired range and plots were made of flow coefficient "K"versus Reynold's number based on orifice diameter, Rd. considerable care was exercised in calibration and results as plotted show a mean deviation from the faired curve of less than 1%. Calibration plots appear as figures 1, 2, and 3.

For use in measuring flow velocities values of test section velocity in feet per second were plotted against differential height of mercury manometer in centimeters for water of 100°F and 150°F. Because the "K" values were essentially constant at the higher Reynold's numbers with the 150°F water and because the difference in water deasity is so slight only the curve for 100°F water is plotted here

as figure 4. Calculations appear in Appendix B .

2. Temperature Measurement

All thermocouples used were copper-constantan, number 36. They were calibrated at three points; ice point, steam point and napthalene vapor point. These were sufficient to cover the required range. Calibration data appears in Appendix C and is plotted in figures 5 and 6. It was originally intended to take three temperature measurements along the heating strip and to measure water temperature both entering and leaving the test section. Since it developed that only the center strip thermocouple could be properly shielded and since increase in water temperature through the test section was barely noticeable, if at all, the two end thermocouples on the heating element and the exit water thermocouple were not used for measurement.

3. Power Measurement

Voltage across the heater element was measured by a potentiometer circuit across the bus bars. As sown by Drucker (2) the error involved in measuring voltage across the bus bars instead of directly across the heater strip is negligible. Calibrated resistances were used in the potentiometer circuit as shown in sketch. The ratio $\frac{9.994}{5013.49} = \frac{Po}{E}$ holds, where Po is potentiometer reading in volts and E the voltage across the bus bars. Because the potentiometer used reads 2x millivolts,

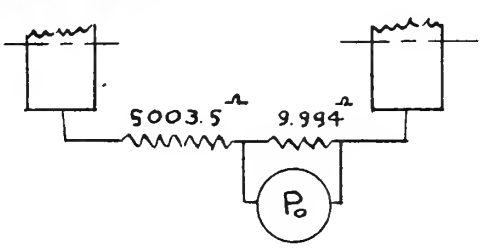

the result is that E = .251 x P where P is the potentiometer reading.

For measuring current, leads were run connecting the potentiometer with a calibrated shunt in the generator circuit. This shunt was labeled 50 m.v. per 1000 amps, and this value was checked against a Bureau of Standards calibration for another shunt used by Osborn and Somma (3) and proved to be exact. Hence for measuring current the value I = 10xP holds where P is the potentiometer reading in 2xm.v.

APPENDIX G

CALCULATED RESULTS

UNITS Run	Ft/ Sec Vel.	Volts E	Amps I	°F T_b	°F T_o	°F ΔT	°F T_w	°F $T_w - T_b$	BTU / HR-FT.^{2} $Q/A \times 10^{-3}$
1	2.73	1.63	129.5	123	179	4.7	174.3	51.3	51.8
1	5	1.295	104.8	118.5	139	3	136	17.5	33.3
3	"	.577	59.5	119	124	1.1	122.9	3.9	8.45
4	"	3.41	260.5	122	251	18.6	232.4	110.4	218
5	"	4.02	305	122	270	25.5	244.5	122.5	301
6	"	4.44	336	122	281	31	250	128	366
7	"	2.83	220.2	112	212	13.5	198.5	86.5	153
8	"	3.43	261	112	246	18.6	227.4	115.4	220
9	"	4.32	325	112	276	29	247	135	345
10	1.7	3.95	297	122	279.5	24.3	255.2	133.2	288
11	"	3.19	241.8	122	265.5	16.2	249.3	127.3	189.1
12	"	2.285	175.5	122	236	8.6	227.4	105.4	98.5
14	"	2.29	176	112	235.5	8.6	226.9	114.9	98.8
15	"	3.3	247	112	265	16.7	248.3	136.3	200
16	"	1.07	88.3	71	118.5	2.3	116.2	45.2	23.2
17	"	.615	51.2	65	86	.9	85.1	20.1	7.73
18	"	4.31	324.5	152	286	29	257	105	343
19	"	2.95	223.5	148	261	14	247	99	161
20	"	1.82	141	142.5	230.5	5.5	225	82.5	63
21	5	5.39	400.6	154	308	45	263	109	530
22	"	3.94	297.7	152.5	280.5	24.3	256.2	103.7	288
23	"	3.32	252	150.5	265	17.5	247.5	97	205.7
24	"	3.32	252	150.5	265	17.5	247.5	97	205.7
25	"	4.39	330	122	289	29.6	259.4	137.4	356
26	"	3.11	238.5	"	239	15.7	223.3	101.3	182
27	"	2.45	192.4	"	198.5	10.05	188.5	66.5	116
28	"	1.875	149.3	"	168	6.3	161.7	39.7	68.8
29	"	1.25	101	"	141	2.9	138.1	16.1	31
30	"	.645	52.5	"	127	.9	126.1	4.1	8.32

TABLE IV.

CALCULATED RESULTS (Continued)

UNITS Run	Ft/ Sec Vel.	Volts E	Amps I	°F T_b	°F T_o	°F ΔT	°F T_w	°F T_w-T_b	BTU/HR-FT.^{2} $Q/A \times 10^{-3}$
31	5	3.82	290.6	112	272	23.0	249	137	272.5
32	"	3.08	238	"	230	15.7	214.3	102.3	180
33	"	2.49	196.5	"	195	10.6	184.4	72.4	120
34	"	3.84	293	"	272.5	23.5	249	137	276.5
35	"	2.04	162	114	170	7.3	162.7	48.7	81.15
36	"	1.604	129	113	146	4.5	141.5	28.5	50.8
37	1.7	3.16	240	112	269.5	16.0	253.5	141.5	272.5
38	"	4.07	306.5	"	286	25.6	260.4	148.4	306.5
39	"	2.535	193.5	"	248	10.5	237.5	125.5	120.4
40	"	1.868	144.7	"	216	5.9	210.1	98.1	66.3
41	"	1.542	122	"	187	4.1	182.9	70.9	46.2
42	"	1.12	90.8	"	149	2.4	146.6	34.6	24.95
43	"	3.92	293.5	122	281	23.5	257.5	135.5	282.5
44	"	2.56	195.2	122	253.5	10.7	242.8	120.8	122.8
45	"	1.883	147	122	221	6.0	215	93	68
46	"	1.47	116.5	120	182	37	178.3	58.3	42.1
47	1	4.22	317.4	122	289	27.5	261.5	139.5	329
48	"	1.871	145	122	240.5	5.9	234.6	112.6	66.6
49	"	1.53	119.5	120	214	4.0	210	90.0	44.85
50	"	3.68	277	122	280	21.0	259	137	250
51	"	3.05	231.8	122	271	14.9	256.1	134.1	173.5
52	"	3.93	297	137.5	281.5	24.0	257.5	120.0	286.5
53	"	2.16	165	122	251	7.6	243.4	121.4	87.5
54	"	2.65	202	120	261.5	11.5	250	130	131.5
55	"	1.015	81.4	124	172	2.0	170	46	20.3
56	"	4.3	322.3	105	286	28.2	257.8	152.8	340
57	"	4.34	326	105	288	29.0	259	154.0	348
58	"	4.585	345	122	294	32.5	261.5	139.5	389
59	"	4.265	288	"	280.5	22.8	257.7	135.7	301
60	"	2.915	221.2	"	266	16.6	249.4	127.4	158
61	"	1.99	152	"	244	6.5	237.5	115.5	74.25
62	"	1.955	151	102	239	6.4	232.6	130.6	72.5
63	"	3.01	228.5	"	268	14.5	253.5	151.5	169
64	"	4.025	303.5	"	286	25.0	261	159.0	300
65	"	5.04	377.5	"	303	39.0	264	162.0	467
66	"	5.02	374.5	82	306	38.4	267.6	185.6	462
67	"	4.34	326	"	290	29.0	261	179.0	347
68	"	3.61	273	"	278	20.5	257.5	175.5	242
69	"	1.95	152	"	222	6.5	215.5	133.5	72.7
70	"	5.46	406.8	76	313	45.1	267.9	191.9	545
71	"	4.075	306	"	258	25.6	262.4	186.4	306
72	"	2.975	226	"	266	14.2	251.8	175.8	165
73	"	2.34	180	"	230.5	9.0	221.5	145.5	103.5
74	"	2.43	184.3	112	257	9.5	247.5	135.5	109.7
75	"	2.38	183.0	82	236	9.45	226.5	144.5	107

BUBBLE POPULATION AND ROOT MEAN CUBE
DIAMETER AT 21 x MAGNIFICATION

Picture No.	Total No. Visible Bubbles	No. and Measured Diameter of Visible Bubbles .1"	.2"	.3"	.4"	Dimensions from Magnified Print ℓ_m	d_m	V_b	V_c	V_d	r_1	r_2	$\frac{Q}{A} = 10^{-3}$	Subcooling
22	21	8	9	2	2	1.66	.232	.138	.364	16.48	.62	.99161	389.0	90°
23	24	10	10	3	1	1.66	.214	.123	.336	16.48	.64	.99252	301.0	"
24	25	13	10	2		1.66	.180	.0727	.282	16.48	.742	.99560	158.0	"
25	30	21	5	4		7.5	.175	.0842	1.24	74.5	.932	.99887	74.2	"
26	21	9	8	4		7.5	.205	.0948	1.282	74.5	.926	.99873	72.5	100°
27	87	68	15	2		7.5	.1575	.178	1.115	74.5	.840	.99761	169.0	"
28	87	65	14	8		3.78	.157	.1774	.57	37.5	.690	.99536	300.0	"
29	27	11	12	4		1.48	.200	.113	.280	14.65	.597	.99230	467.0	"
30	34	14	15	5		1.66	.192	.1255	.3015	16.48	.584	.99240	462.0	130°
31	20	10	6	4		1.67	.205	.092	.324	16.58	.717	.99444	347.0	"
32	18	10	6	2		1.8	.184	.0585	.313	17.82	.814	.99673	242.0	"
33	12	5	5	1	1	7.5	.225	.0715	1.598	74.5	.956	.99996	72.7	"

TABLE V

Calculations to Check Validity of Non-Boiling Points

$D = 4r_h$;

$$Re = \frac{\rho VDx3600}{\mu}; \quad Pr = \frac{C_p \mu}{k}; \quad Nu = \frac{Q/A \times D}{\Delta t \times k};$$

$$J = \frac{Nu}{Pr^{1/3} Re}\left(\frac{\mu_w}{\mu_b}\right)^{a/4} = \frac{h}{CpG}(Pr)^{2/3}\left(\frac{\mu_w}{\mu_b}\right)^{0.14}$$

Run	V	tw	tb	Δt	$\frac{Q}{A} \times 10^{-3}$	Cp	k	ρb	μb	μw	$Re_x 10^{-3}$	Pr	$(Pr)^{\frac{1}{3}}$	Nu	$(\mu_b/\mu_w)^{a/4}$	J $\times 10^{5}$
1	2.73	174.3	123	51.3	51.8	.9994	.3745	61.6	1.318	.877	30.9	3.51	1.52	181	1.058	366
2	5	136	118.5	17.5	33.3	.9979	.3726	61.6	1.373	1.177	54.2	3.68	1.545	344	1.022	402
3	5	122.9	119.0	3.9	8.45	.9977	.3728	61.6	1.366	1.318	54.6	3.66	1.542	390	1.008	462
7	5	198.5	112	86.5	153.0	1.0000	.3698	61.9	1.460	.740	51.2	3.96	1.58	322	1.100	362
16	1.7	116.2	71	45.2	23.0	.9975	.3478	62.1	2.343	1.407	10.9	6.75	1.89	98.5	1.073	441
17	1.7	85.1	65	20.1	7.73	.9975	.3435	62.1	2.552	1.965	16.5	7.44	1.95	75.2	1.038	226
27	5	188.5	122	66.5	116.0	1.000	.3741	61.6	1.330	.796	56.0	3.56	1.525	314.0	1.075	342
28	5	161.7	122	39.7	68.8	.9988	.3741	61.6	1.330	.956	56.0	3.56	1.525	312.0	1.047	350
29	5	138.1	122	16.1	31.0	.9981	.3741	61.6	1.330	1.157	56.0	3.56	1.525	346.0	1.020	398
30	5	126.1	122	4.1	8.32	.9979	.3741	61.6	1.330	1.283	56.0	3.56	1.525	364.0	1.000	426
33	5	184.4	112	72.4	120.0	.9994	.3698	61.9	1.460	.818	51.2	3.96	1.58	302	1.084	344
35	5	162.7	114	48.7	81.1	.9987	.3706	61.7	1.433	.954	52.0	3.87	1.57	330.2	1.06	381
36	5	141.5	113	28.5	50.8	.9979	.3702	61.9	1.447	1.115	51.8	3.90	1.574	324.0	1.037	384
40	1.7	210.1	112	98.1	66.3	1.0005	.3698	61.9	1.460	.702	17.4	3.96	1.584	123.0	1.105	405
41	1.7	182.9	112	70.9	46.2	.9994	.3698	61.9	1.460	..823	17.4	3.96	1.584	118.7	1.084	395
42	1.7	146.6	112	34.6	24.95	.9980	.3698	61.9	1.460	1.076	17.4	3.96	1.584	131.4	1.044	455
46	1.7	178.3	120	58.3	42.10	.9996	.3733	61.6	1.353	.852	18.7	3.64	1.540	130.0	1.067	413
49	1.0	210.0	120	90.0	44.85	1.0008	.3733	61.6	1.353	.702	11.0	3.64	1.540	89.9	1.097	485
55	1.0	170.5	124	46.0	20.3	.9993	.3757	61.5	1.306	.902	11.4	3.48	1.515	79.0	1.052	433

TABLE VI.

APPENDIX H

SUPPLEMENTARY DISCUSSION

Method of Determining Twall

Formula used to determine the temperature of the heater strip on the water side was derived by Drucker (2). In this derivation it was assumed that all of the electrical energy put into the heater strip is transferred as heat to the circulating water. Both the thermal conductivity k and the electrical resisivity ρ are considered linear functions of the temperature and are plotted as figures XII and XIII respectively. The formula is:

$$Tw = To - \frac{\Delta y^2 m}{(1+\alpha To)(1+\beta To)} - \frac{\Delta y^4 m^2}{6}\left[\frac{3\alpha+4\alpha\beta To+\beta}{(1+\alpha To)^3(1+\beta To)^3}\right]$$

$$\text{now } m = G\left(\frac{dE}{dx}\right)^2 \Big/ 2\rho_o k_o \qquad \text{and } To - Tw = \Delta T$$

$$\text{but } E = IR$$

$$dE = I\rho_m \frac{dx}{A}$$

$$\frac{dE}{dx} = \frac{I\rho m}{A} = \frac{I\rho_m}{\Delta y b}$$

$$\text{also } \rho_o k_o(1+\alpha T_o)(1+\beta T_o) = \rho k$$

Thus we may write after substitution and cancellation

$$\Delta T = \frac{GI^2\rho m^2}{2\rho k b^2} + \frac{6GI^4\rho_m{}^4}{\rho^2_k\, {}^2_b{}^4}\left[\frac{3\alpha+4\alpha BT_o+B}{(1+\alpha T_o)(1+\beta T_o)}\right]$$

Fig. XIV originally plotted by Drucker (2) shows the temperature distribution through our heating element for a T_o of 400°F. This figure was integrated to find the mean temperature. This value yielded the following relationship which we assume holds for various assumed values of ΔT and To:

$$T_m = T_w + \frac{71}{105} \Delta T$$

values of T_m obtained from this relationship were used to obtain ρ_m.

Curves were plotted for values of I vs ΔT by assuming a value for T_o and several increments of ΔT. Only the first term in the expression for ΔT was used since numerical calculation indicated that the effect of the second term was only of the order of 1%, which amounts to only a fraction of one degree in the range with which we are concerned. Values were calculated for T_o from 150°F to 350°F and the curves for all T_os are so close to being superimposed that a single curve is within the accuracy of our data. A plotted curve of ΔT vs I appears as fig. XV .

Correlation of Data

To determine the validity of the data obtained, both the non-boiling runs and the boiling runs were correlated. The non-boiling data was correlated with the Sieder and Tate equation;

$$\frac{hD}{k} = .027 \left(\frac{DG}{\mu}\right)^{0.8} \left(\frac{C_p \mu}{k}\right)^{1/3} \left(\frac{\mu_b}{\mu_w}\right)^{0.14}$$

This was plotted in the form of J vs Re, fig. XVI, where $J = \left(\frac{h}{C_p G}\right)\left(\frac{C_p \mu}{k}\right)^{2/3}\left(\frac{\mu_w}{\mu_b}\right)^{0.14}$. Most of the data plots slightly above this line which may be explained by the fact that the Sieder and Tate equation was obtained with a value of $\frac{L}{D}$ above 32, where L is the heated length and D the diameter. The equivalent diameter for this investigation was .0672 feet, giving an $\frac{L}{D}$ of 5.3. As $\frac{L}{D}$ decreases to low values, h increases rapidly. This would result in higher values of J than those predicted by the Sieder and Tate equation. It is also noted that the Sieder and Tate equation is based on a cylindrical heating surface and the element used here is a flat plate.

The boiling data was correlated with that of Dew (7) and Carl and Picornell (7) by plotting $\frac{Q}{A}$ vs $\Delta T_{SAT.}$, fig. XVII. At high heat flux densities our data correlates well yielding an equation in the straight line portion of the curve which is $\frac{Q}{A} = 0.135\ (\Delta T_{SAT})^{3.86}$.

At the lower heat flux densities velocity is observed to have an effect on the curve. The higher velocity points plot at a higher $\frac{Q}{A}$ for the same ΔT_{SAT}.

APPENDIX I

ORIGINAL DATA - 21 April 1951

Run No.	CM HG ΔH	ORIFICE	POTEN READING T_b	T_a	T_o	I	E	Pict.No.
1	14.3	"A"	4.1	6.83	6.83	12.95	6.5	
2	40	"B"	3.9	4.88	4.88	10.48	5.17	
3	"	"	3.91	4.15	4.15	5.95	2.3	
4	"	"	4.05	10.55	10.55	26.05	13.6	
5	"	"	4.05	11.62	11.62	30.5	16.0	
6	"	"	4.05	12.21	12.21	33.6	17.7	
7	"	"	3.6	8.53	8.53	22.02	11.27	
8	"	"	3.6	10.3	10.3	26.1	13.65	
9	"	"	3.6	11.96	11.96	32.5	17.2	
10	4.5	"	4.05	12.16	12.16	29.7	15.75	
11	"	"	4.05	11.38	11.36	24.18	12.70	
12	"	"	4.05	9.78	9.78	17.55	9.10	
13	"	"	3.6	12.75	12.75	29.7	15.7	
14	"	"	3.6	9.75	9.75	17.6	9.12	
15	"	"	3.6	11.35	11.35	24.7	13.14	
16	"	"	1.7	3.9	3.9	8.83	4.26	
17	"	"	1.46	2.4	2.4	5.12	2.45	

ORIGINAL DATA - 23 April 1951

Run No.	CM HG ΔH	ORIFICE	POTEN READING T_b	T_a	T_o	I	E	Pict.No.
18	4.5	"B"	5.5	12.5	12.5	32.45	17.2	3
19	4.5	"	5.3	11.1	11.1	22.35	11.75	4
20	4.5	"	5.03	9.5	9.5	14.1	7.25	5
21	40	"	5.6	13.7	13.7	40.06	21.44	6
22	40	"	5.55	12.2	12.2	29.77	15.7	7
23	40	"	5.45	11.35	11.35	25.20	13.26	8
24	40	"	5.45	11.35	11.35	25.20	13.26	9

TABLE VII.

ORIGINAL DATA - 27 April, 1951

Run No.	CM HG ΔH	ORIFICE	Poten. Reading T_b	T_a&T_o	I	E	Pict.No.	Movie
25	40	"B"	4.06	12.65	33.0	17.5		
26	"	"	"	9.97	23.85	12.38		
27	"	"	"	7.87	19.24	9.77		
28	"	"	"	6.36	14.93	7.47		
29	"	"	"	5.05	10.10	4.98		
30	"	"	"	4.35	5.25	2.56		
31	"	"	3.6	11.75	29.06	15.22		
32	"	"	"	9.5	23.8	12.27		
33	"	"	"	7.7	19.65	9.94		
34	"	"	"	11.75	29.3	15.31	10	
35	"	"	3.7	6.42	16.2	8.15		
36	"	"	3.6	5.3	12.9	6.4		
37	4.5	"	"	11.6	24.0	12.6		
38	"	"	"	12.5	30.65	16.2		
39	"	"	"	10.45	19.35	10.1	11	
40	"	"	"	8.7	14.47	7.44	12	
41	"	"	"	7.3	12.20	6.15		
42	"	"	"	5.45	9.08	4.46		Movie
43	"	"	4.06	12.2	29.35	15.6	13	#3,#4
44	"	"	"	10.75	19.52	10.2		
45	"	"	"	8.95	14.7	7.5		#5
46	"	"	3.96	7.03	11.65	5.85		
47	9	"C"	4.06	12.65	31.74	16.82		#6
48	"	"	"	10.05	14.5	7.46		#7
49	"	"	3.96	8.7	11.95	6.10	14	
50	"	"	4.06	12.15	27.7	14.65	15	
51	"	"	"	11.68	23.18	12.17	16	
52	"	"	4.88	12.26	29.7	15.67	17	
53	"	"	4.06	10.6	16.5	8.6		
54	"	"	3.95	11.17	20.2	10.55		
55	"	"	4.15	6.53	8.14	4.05		

ORIGINAL DATA - 7 May, 1951

Run No.	CM HG Δ H	ORIFICE	Poten Reading T_b	T_a&T_o	I	E	Pict.No.	
56	9	"C"	3.25	12.5	32.23	17.15	20	
57	"	"	3.25	12.6	32.6	17.3	21	
58	"	"	4.06	12.95	34.5	18.37	22	
59	"	"	"	12.2	28.8	17.0	23	
60	"	"	"	11.4	22.12	11.62	24	
61	"	"	"	10.2	15.2	7.92	25	
62	"	"	3.1	9.96	15.1	7.8	26	
63	"	"	"	11.5	22.85	12.0	27	
64	"	"	"	12.5	30.35	16.05	28	
65	"	"	"	13.45	37.75	20.1	29	
66	"	"	2.22	13.6	37.45	20.0	30	
67	"	"	"	12.75	32.6	17.3	31	
68	"	"	"	12.06	27.3	14.4	32	
69	"	"	"	9.05	15.2	7.78	33	
70	"	"	1.93	14.0	40.68	21.77	34	
71	"	"	"	12.6	30.6	16.25	35	
72	"	"	"	11.4	22.6	11.86	36	
73	"	"	"	9.5	18.0	9.33	37	Movie
74	"	"	3.6	10.9	18.43	9.68		8
75	"	"	2.22	9.8	18.3	9.50		9

APPENDIX J

BIBLIOGRAPHY

1. A.S.M.E. Power Test Codes, Part 5, Chapter 4.
2. Drucker, Eugene E., "The Design of Apparatus For a Study of Bubble Formation in Surface Boiling", S.M. Thesis in Mechanical Engineering, M.I.T., 1950.
3. Osborn, P. V. and E. H. Somma, "Heat Transfer at High Rates to Water Flowing in Tubes with Surface Boiling", S.M. Thesis in Mechanical Engineering, M.I.T., 1950.
4. Mullin, F. J. and Malherbe, P. N., "Heat Transfer With Surface Boiling to Water Under Pressure Flowing at Low Velocities", S.M. Thesis in Mechanical Engineering, M.I.T., 1951.
5. Rohsenow, W. M. and Clark, J. A., "A Study of The Mechanism of Boiling Heat Transfer" paper No. 50-A-60 presented before Heat Transfer Division of ASME, Dec., 1950.
6. Whiston, William B., "Photographic Techniques Applied to the Mechanism of Surface Boiling in Subcooled Liquids", S.B. Thesis in Chemical Engineering, M.I.T., 1951.
7. Dew, Jess E., "Local Boiling of Water in an Annulus", S.M. Thesis in Chemical Engineering, M.I.T., 1948.
8. McAdams, W.H., Kennel, W. E., Minden, C. S., Rudolf, C., Picornell, P. M., Dew, J. E., "Heat Transfer at High Rates to Water with Surface Boiling" Industrial and Engineering Chemistry, Vol. 41, Sept. 1949, p. 1945-1953.

BIBLIOGRAPHY

9. Kreith, F. and M. Summerfield, "Investigation of Heat Transfer at High Heat-Flux Densities: Experimental Study with Water of Friction Drop and Forced Convection with and without Surface Boiling in Tubes", Progress Report No. 4-68, Jet Propulsion Lab., C.I.T., 1948.

10. Minden, C. S., "Heat Transfer to Water Flowing in an Annulus", S.M. Thesis in Chemical Engineering, M.I.T., 1947.

11. Keenan, J. H. and Keyes, F. G., "Thermodynamic Properties of Steam", John Wiley and Sons, Inc., New York, 1936.

12. McAdams, W. H., "Heat Transmission", 2nd Edition, McGraw Hill Book Co., New York, 1942.

FLOW COEFFICIENT VS REYNOLDS NO

ORIFICE "A" - D = 7.81"

CALIBRATED AT M.I.T. 30 JAN, 1951

P. O. Chapman

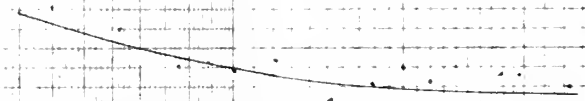

.8

K

.7

FIG I.

10^4 2 3 4 5 6 7 8 9 10^5 2 3

R_d

FLOW COEFFICIENT VS REYNOLDS NO

ORIFICE "B" DIA = .465"

CALIBRATED AT M.I.T. 30 JAN, 1951

P. O. Chapman

.6

K

.5

FIG. II.

10^4 2 3 4 5 6 7 8 9 10^5 2

R_d

FLOW COEFFICIENT VS REYNOLDS NO.

ORIFICE "C" DIA = .303"

CALIBRATED AT M.I.T. 31 JAN. 1951

P.O. Chapman

.6

K

.5

10^4 2 3 4 5 6 7 8 9 10^5

R_d

FIG. III

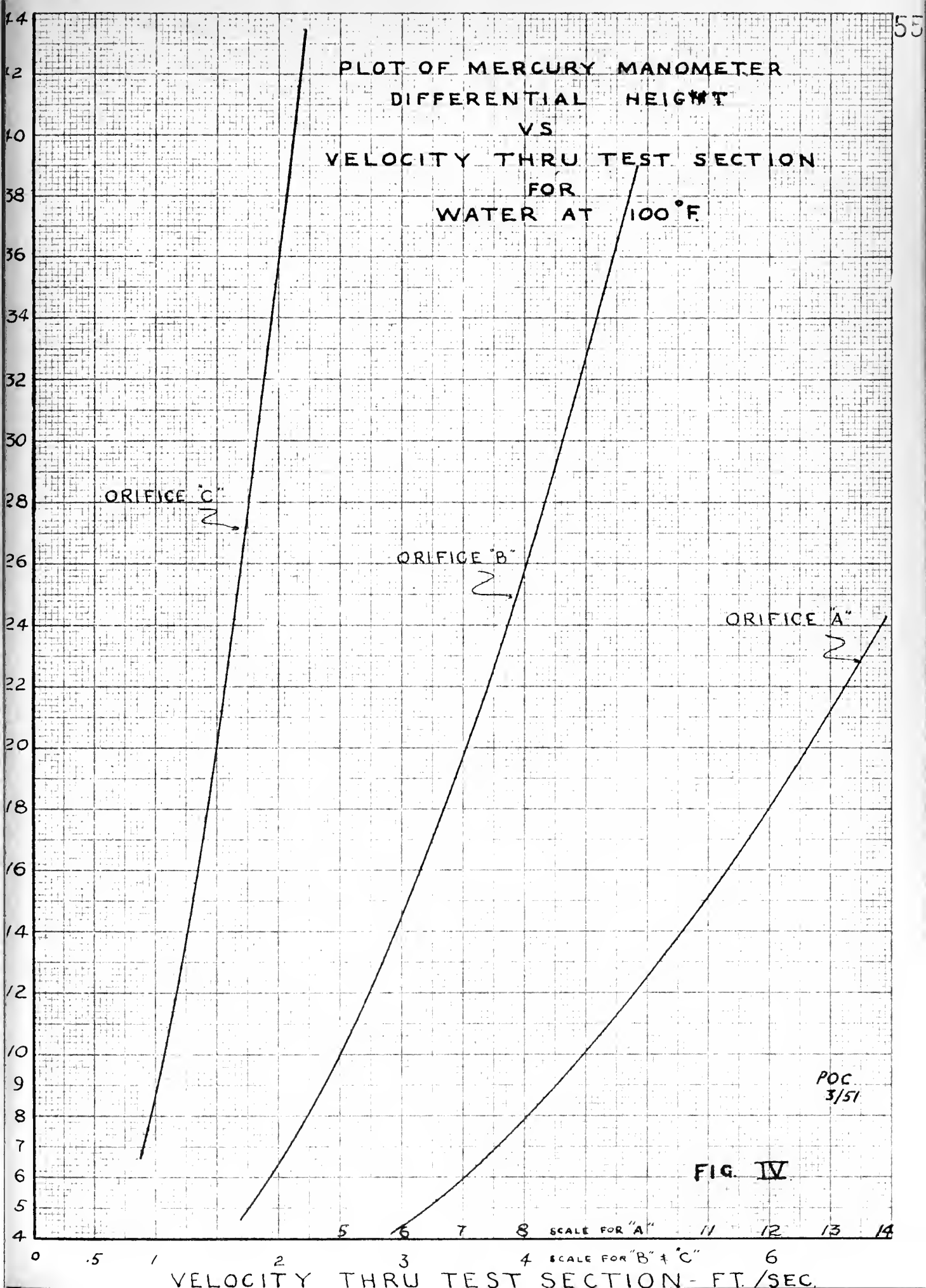
PLOT OF MERCURY MANOMETER
DIFFERENTIAL HEIGHT
VS
VELOCITY THRU TEST SECTION
FOR
WATER AT 100°F.
ORIFICE "C"
ORIFICE "B"
ORIFICE "A"
POC
3/51
FIG. IV
SCALE FOR "A"
SCALE FOR "B" & "C"
VELOCITY THRU TEST SECTION - FT./SEC.

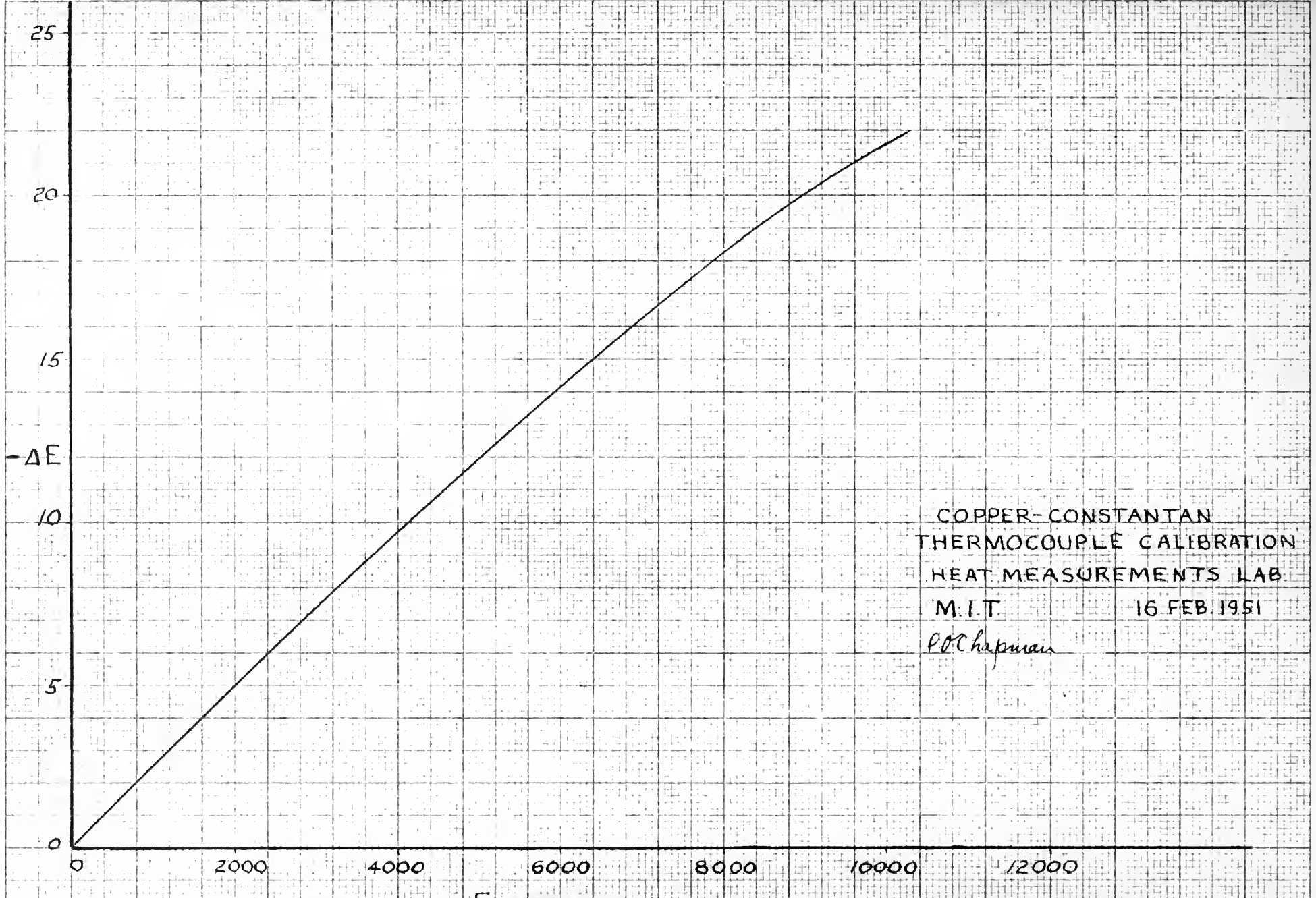
25
20
15
-ΔE
10
5
0
0
2000
4000
6000
8000
10000
12000
E OBSERVED, μ VOLTS
COPPER-CONSTANTAN
THERMOCOUPLE CALIBRATION
HEAT MEASUREMENTS LAB.
M.I.T. 16 FEB. 1951
P.O. Chapman

FIG. V.

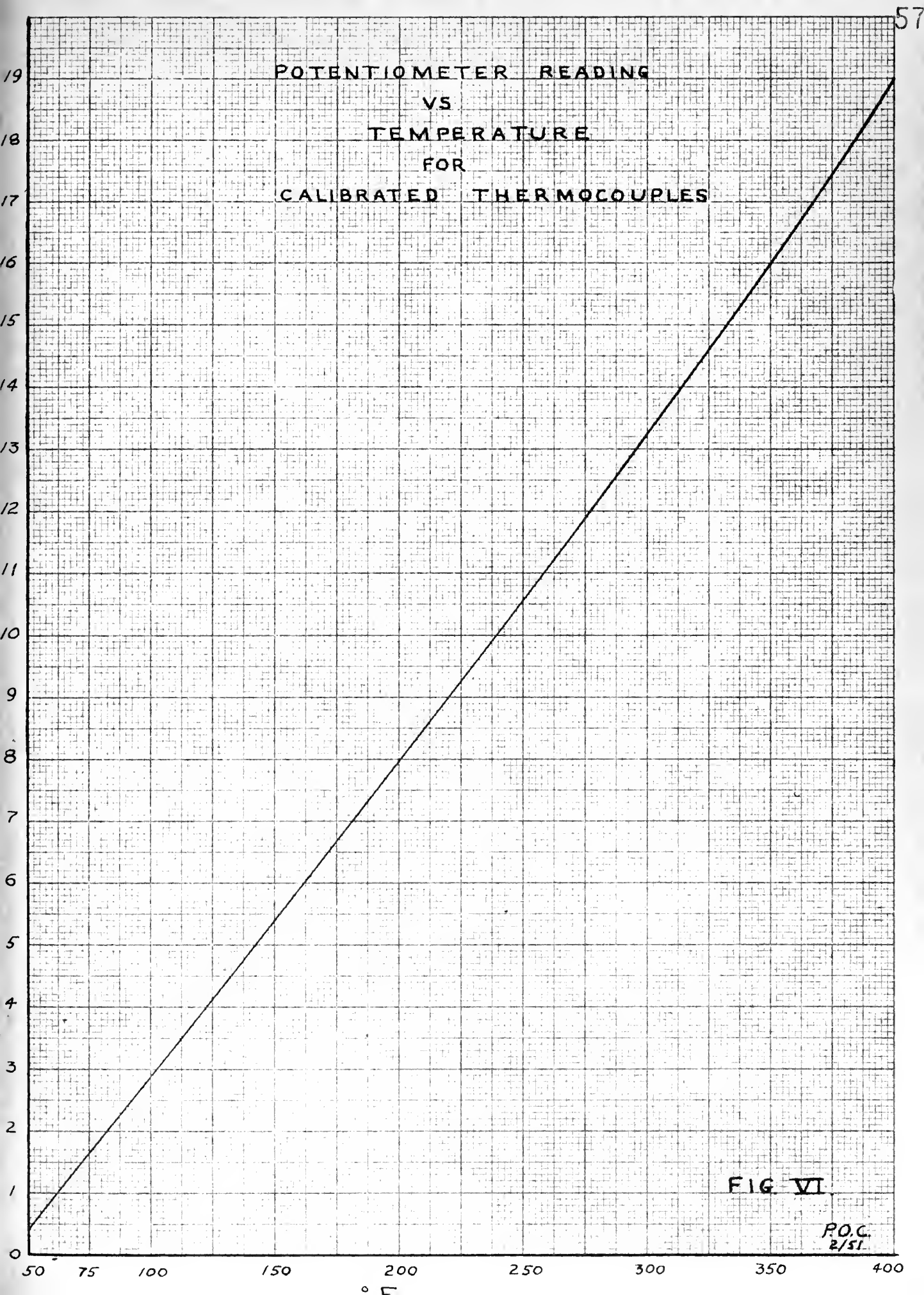

FIG VI

P.O.C.
2/51

FLOW CIRCUIT

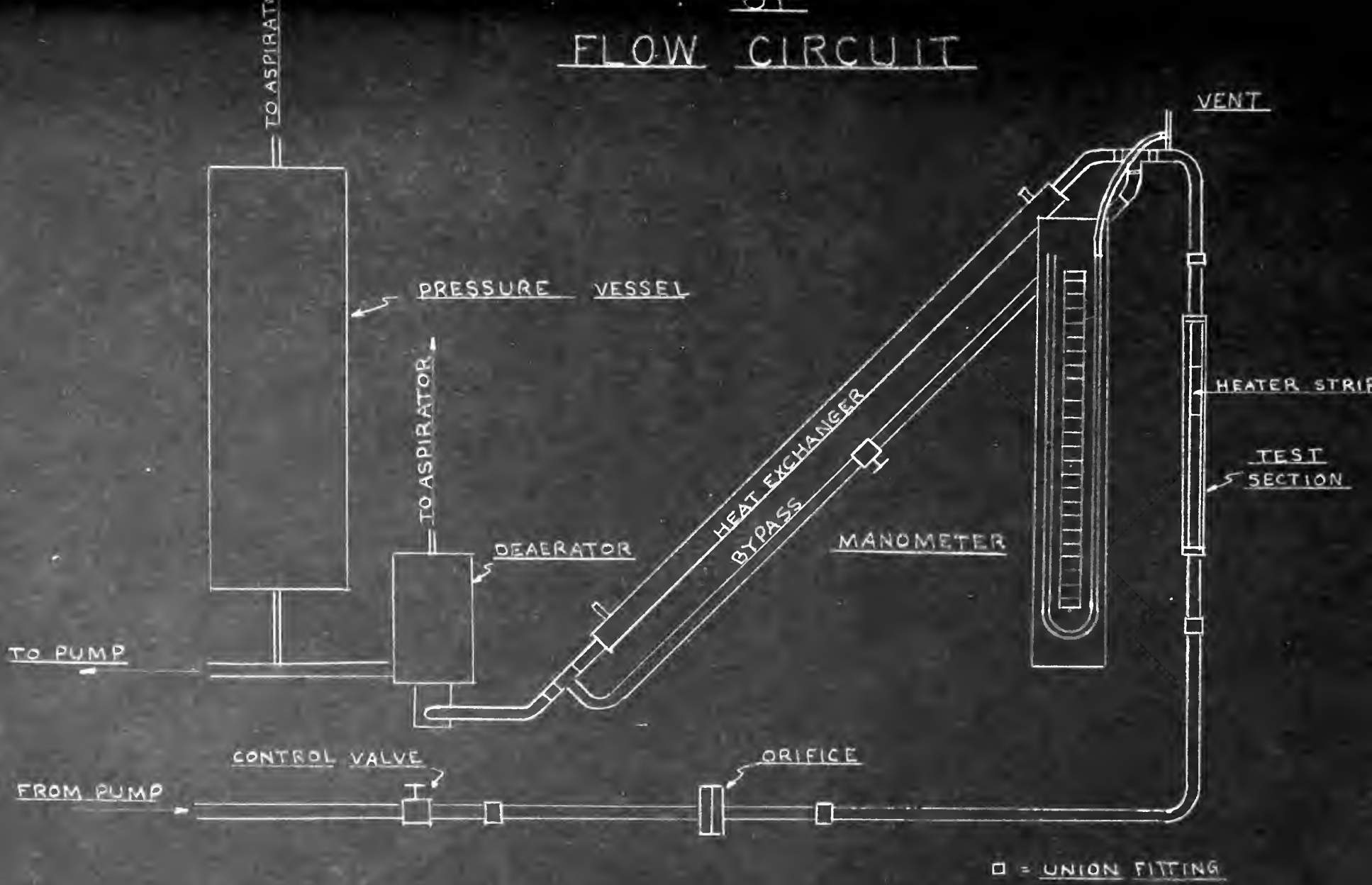

FIG VII

N.P.G.
5/51

PHOTOGRAPH OF APPARATUS SET-UP

FIG. VIII

PHOTOGRAPH OF APPARATUS SET-UP

FIG. VIII

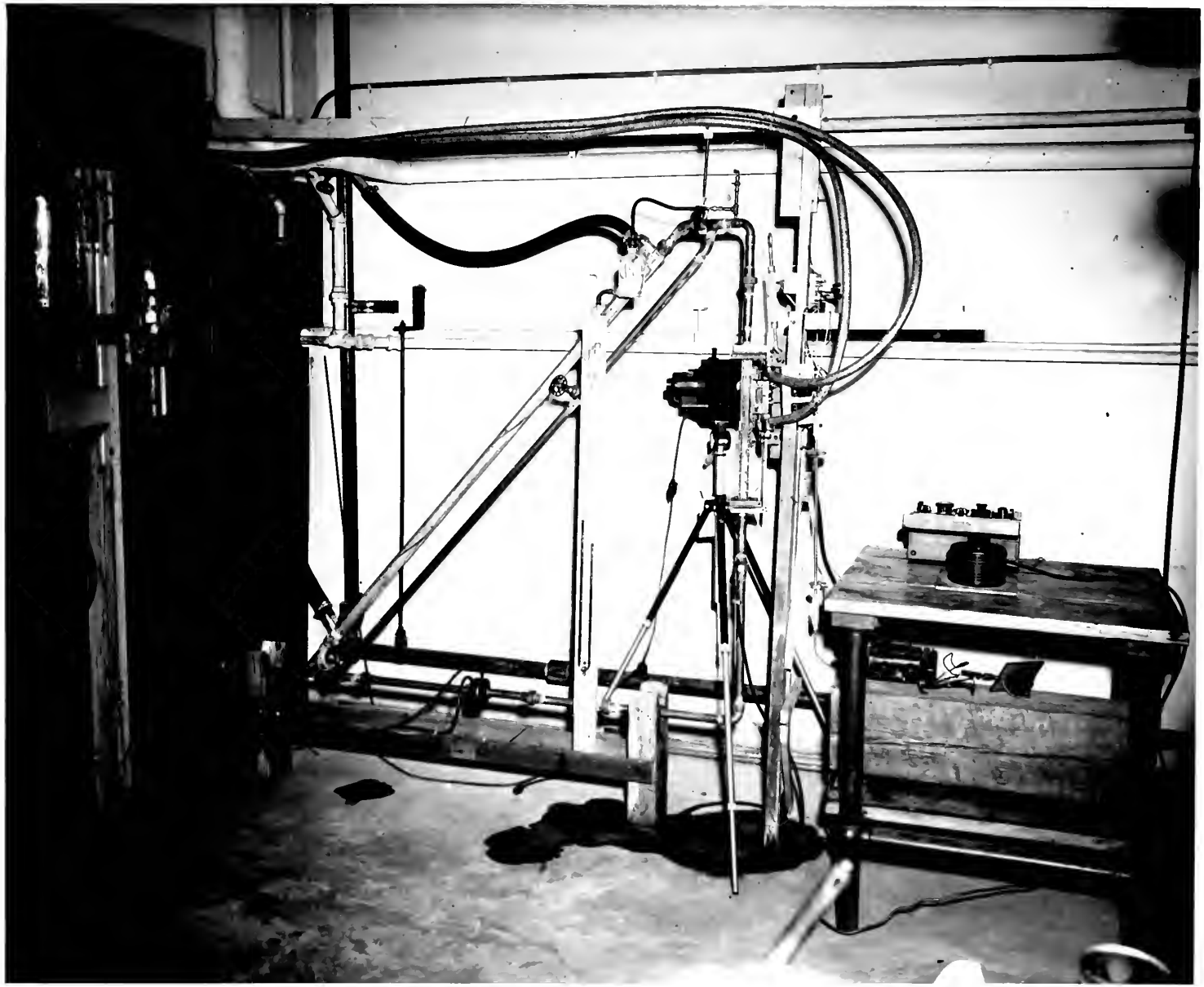

PHOTOGRAPH OF POWER SUPPLY

FIG. VIII-A

PHOTOGRAPH OF POWER SUPPLY

FIG. VIII-A

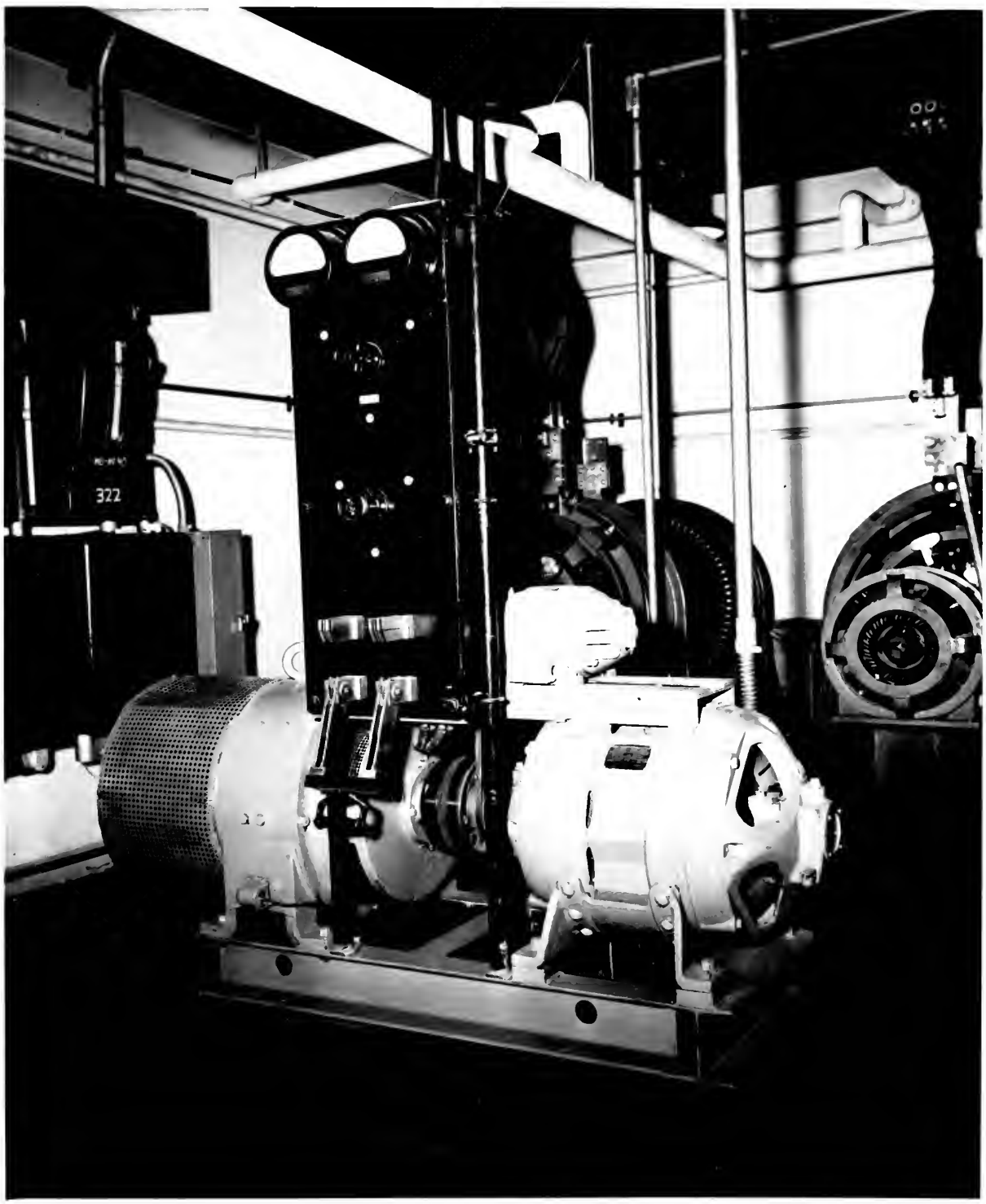
322

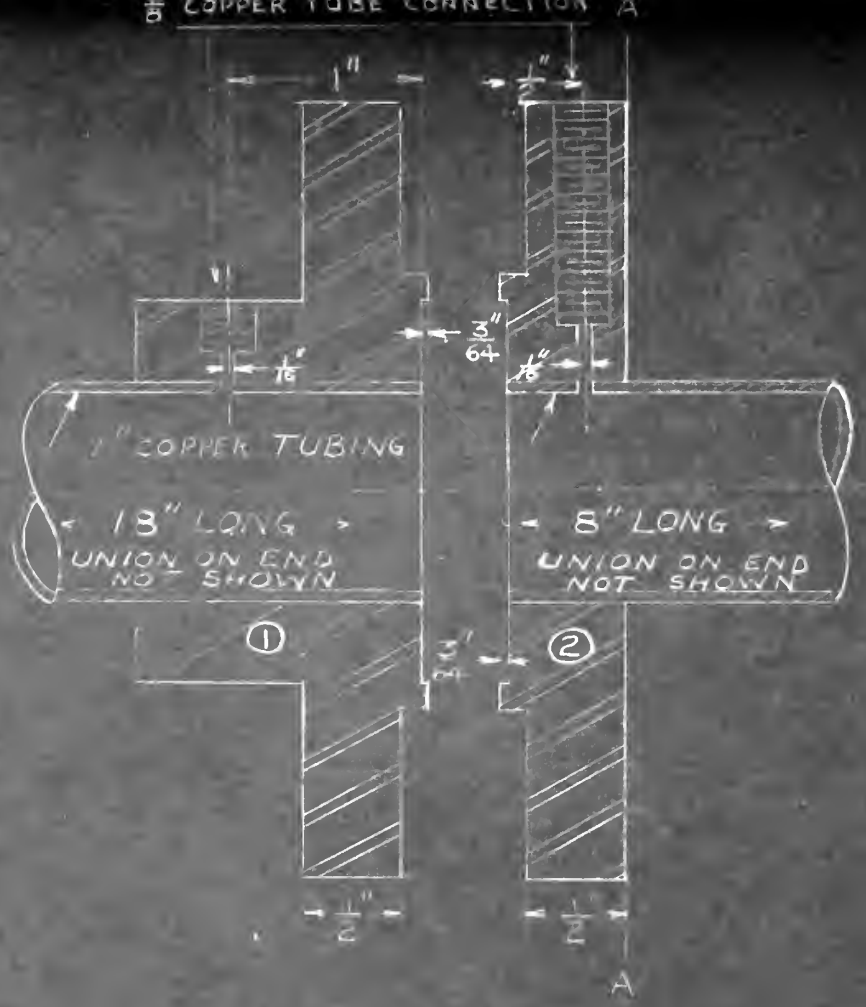

ORIFICE SECTION

PIECE ① - MAKE ONE - STEEL
PIECE ② - MAKE ONE - "
SILVER BRAZE COPPER TO STEEL

PIECE ③ - MAKE THREE IN ALL
1 AT . INSIDE DIA. STAINLESS STEEL
1 AT . " " "
1 AT . " " "

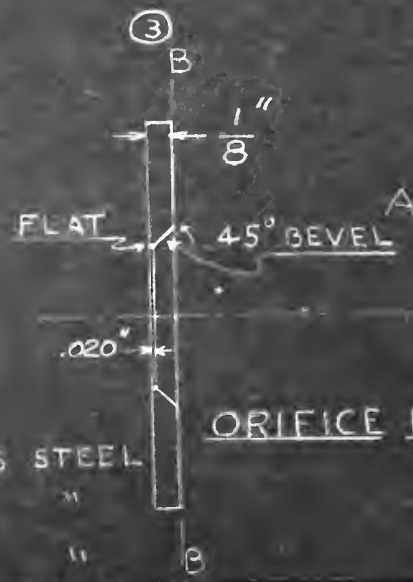

ORIFICE PLATE

FIG. IX

P.O.C.
5/51

SKETCH OF DEAERATOR

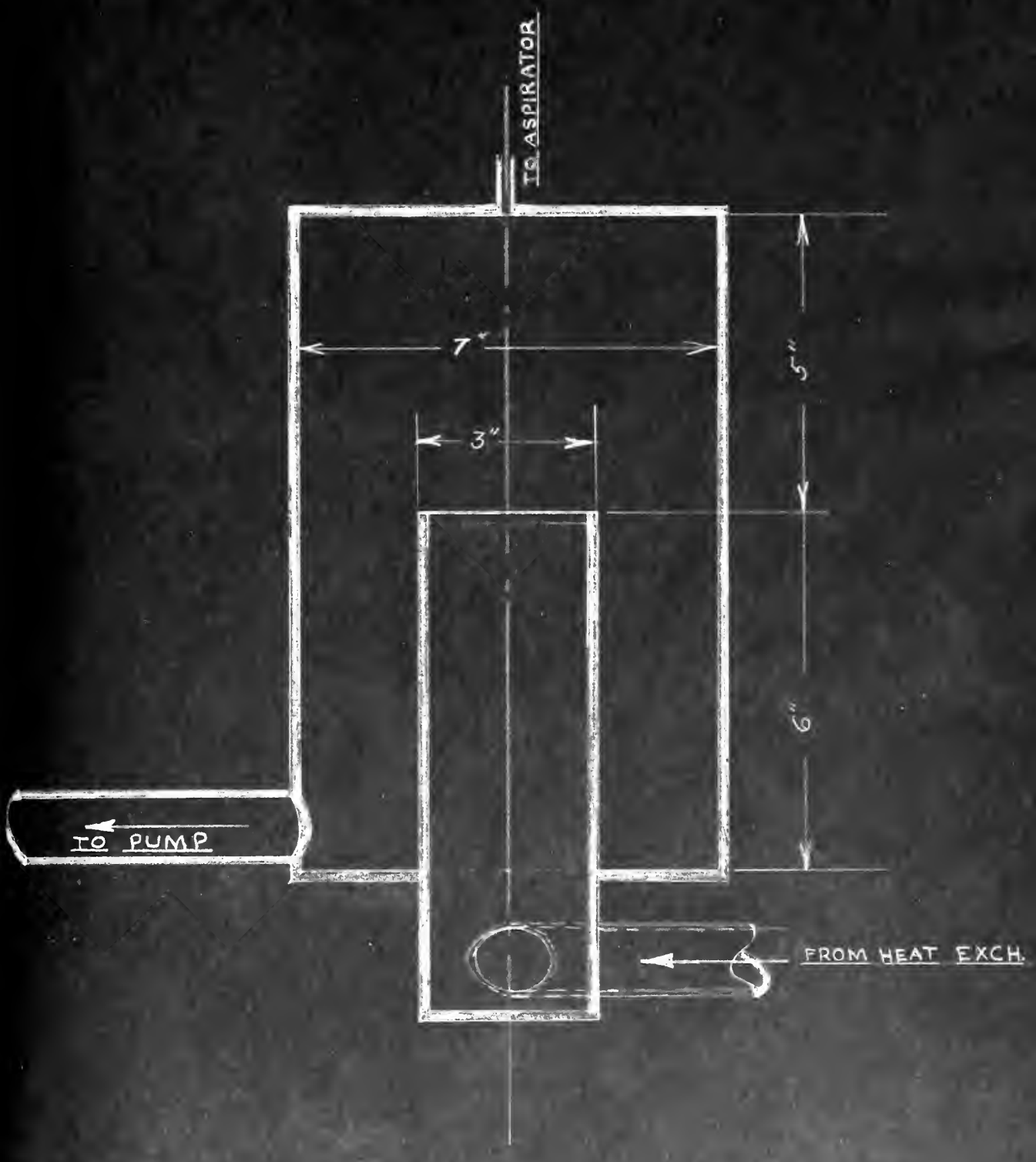

FIG. X

N.F.G.
5/51

SCHEMATIC DIAGRAM OF AIR HEATER

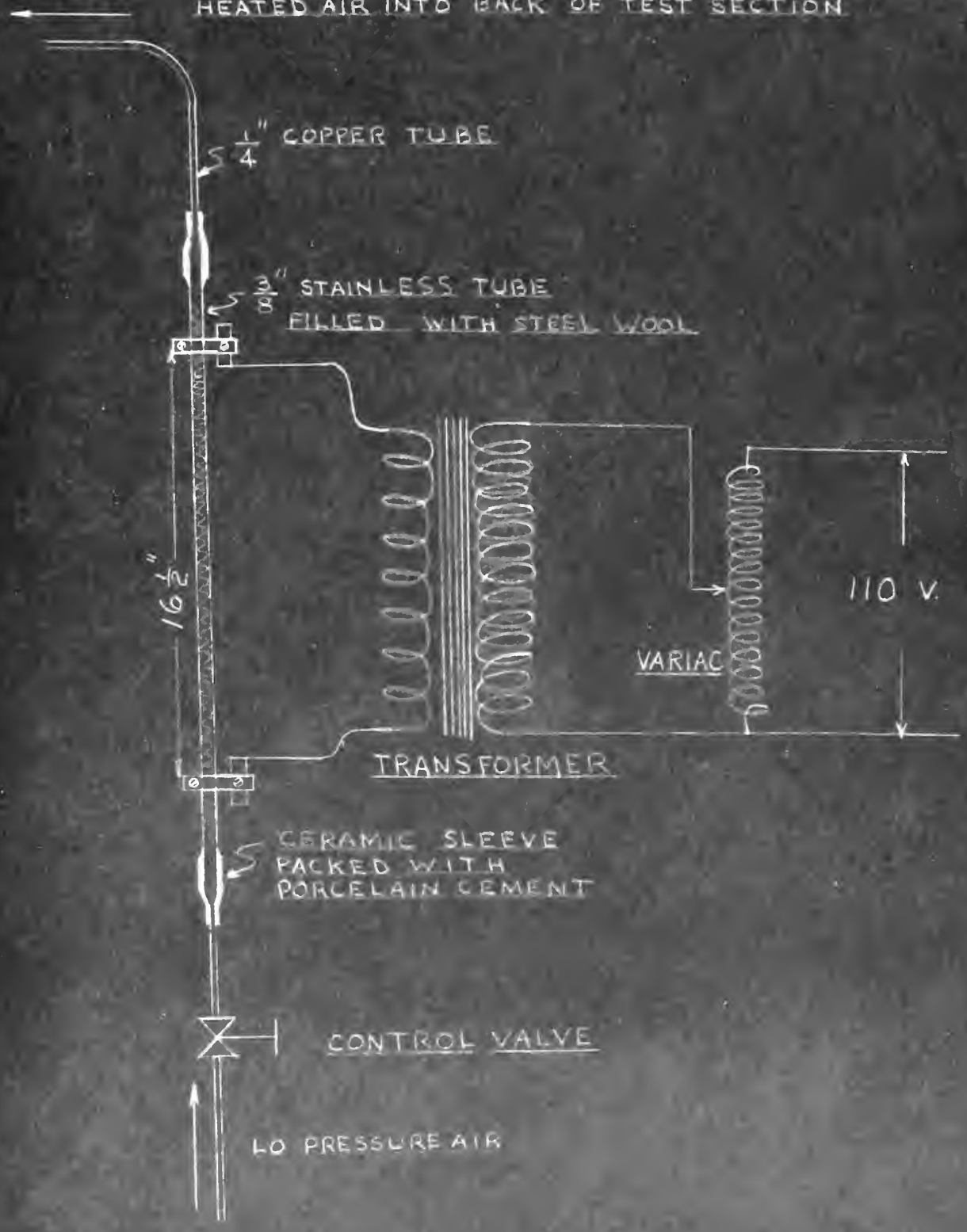

FIG. XI

THERMAL CONDUCTIVITY vs TEMPERATURE FOR STAINLESS-STEEL TYPE 304

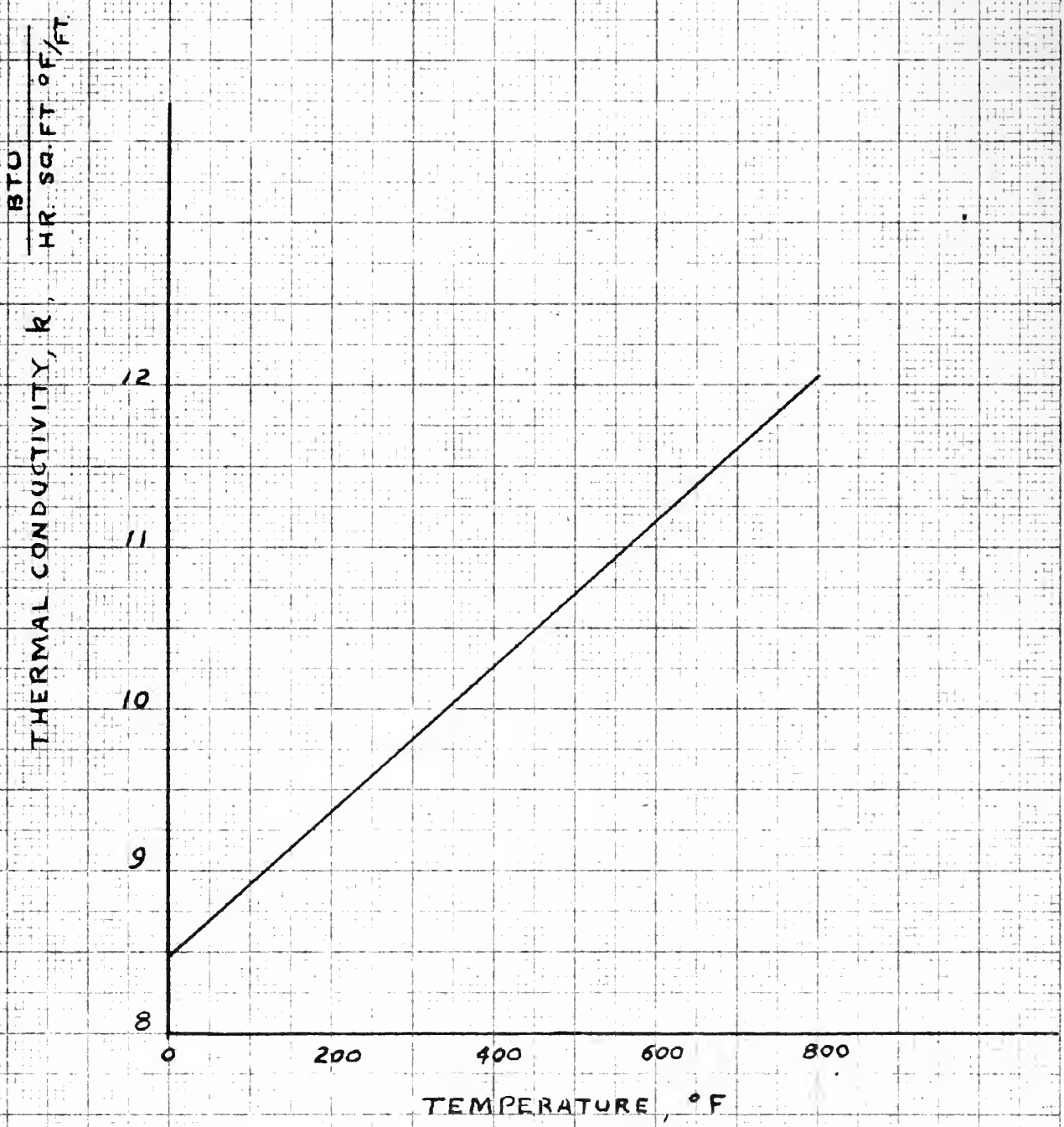

FIG. XII.

EED/POC
5/51

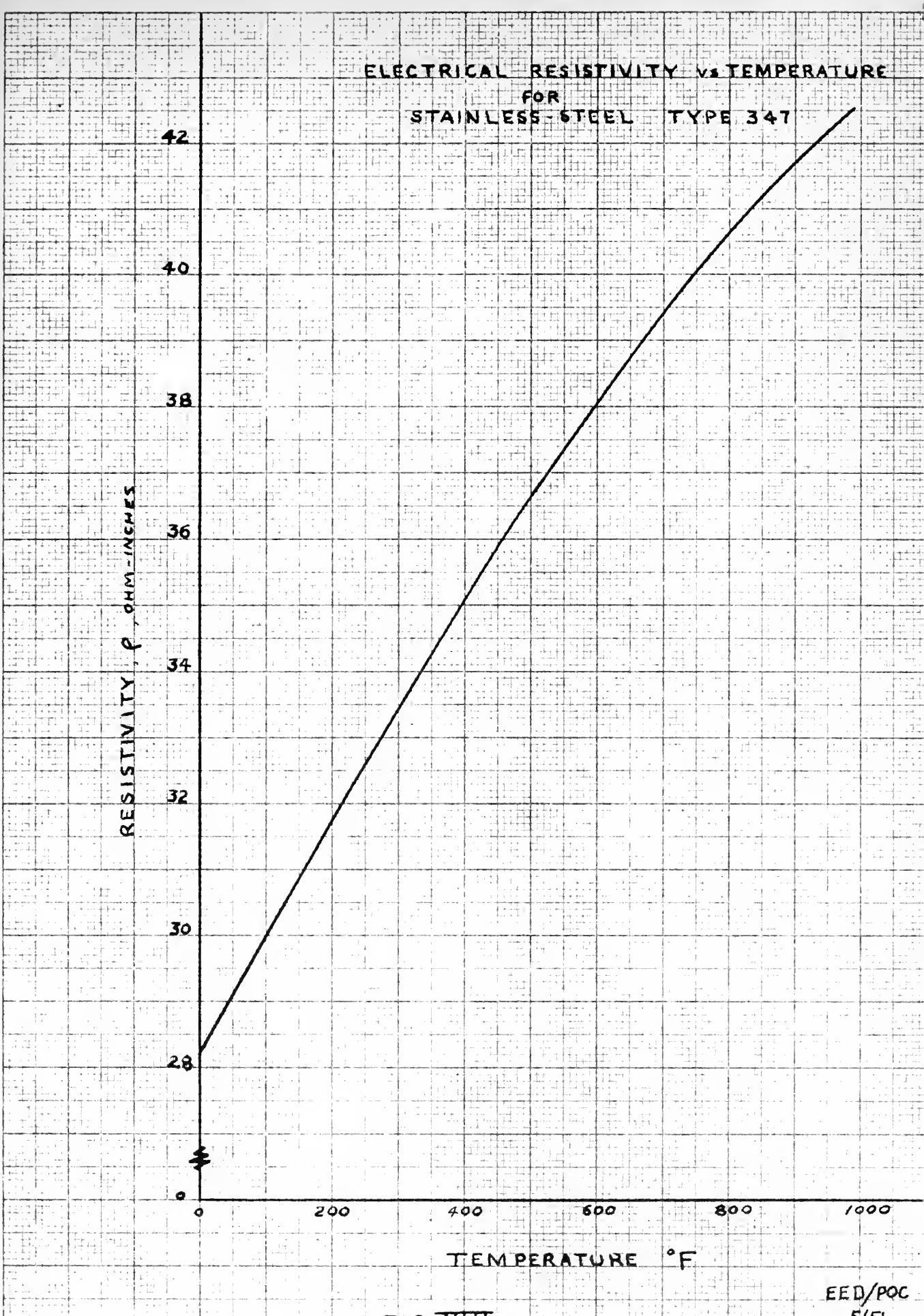

FIG. XIII

EED/POC
5/51

TEMPERATURE DISTRIBUTION THROUGH HEATING ELEMENT FOR INSULATED WALL TEMP. OF 400°F.

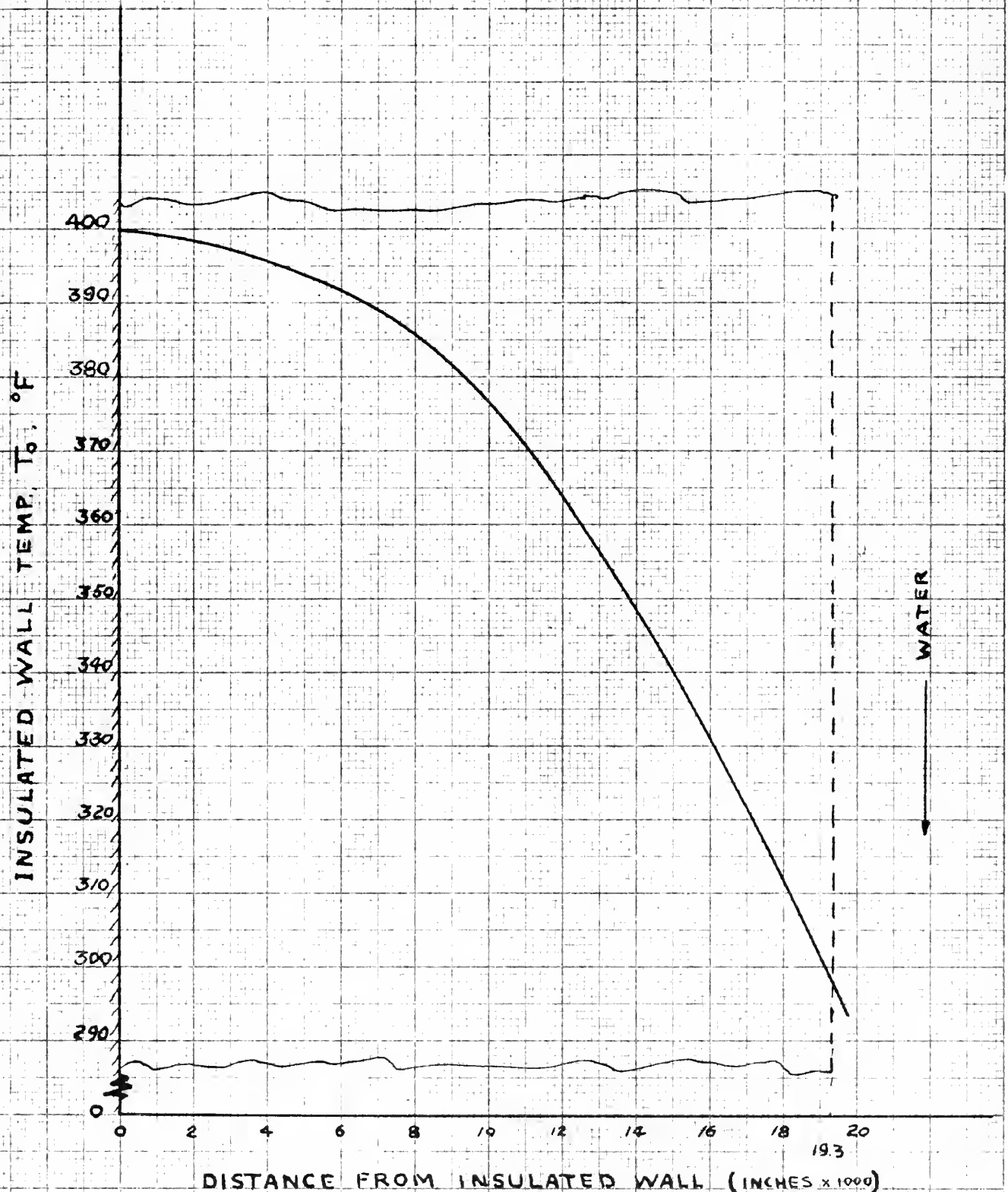

FIG. XIV

EED/POC
5/51

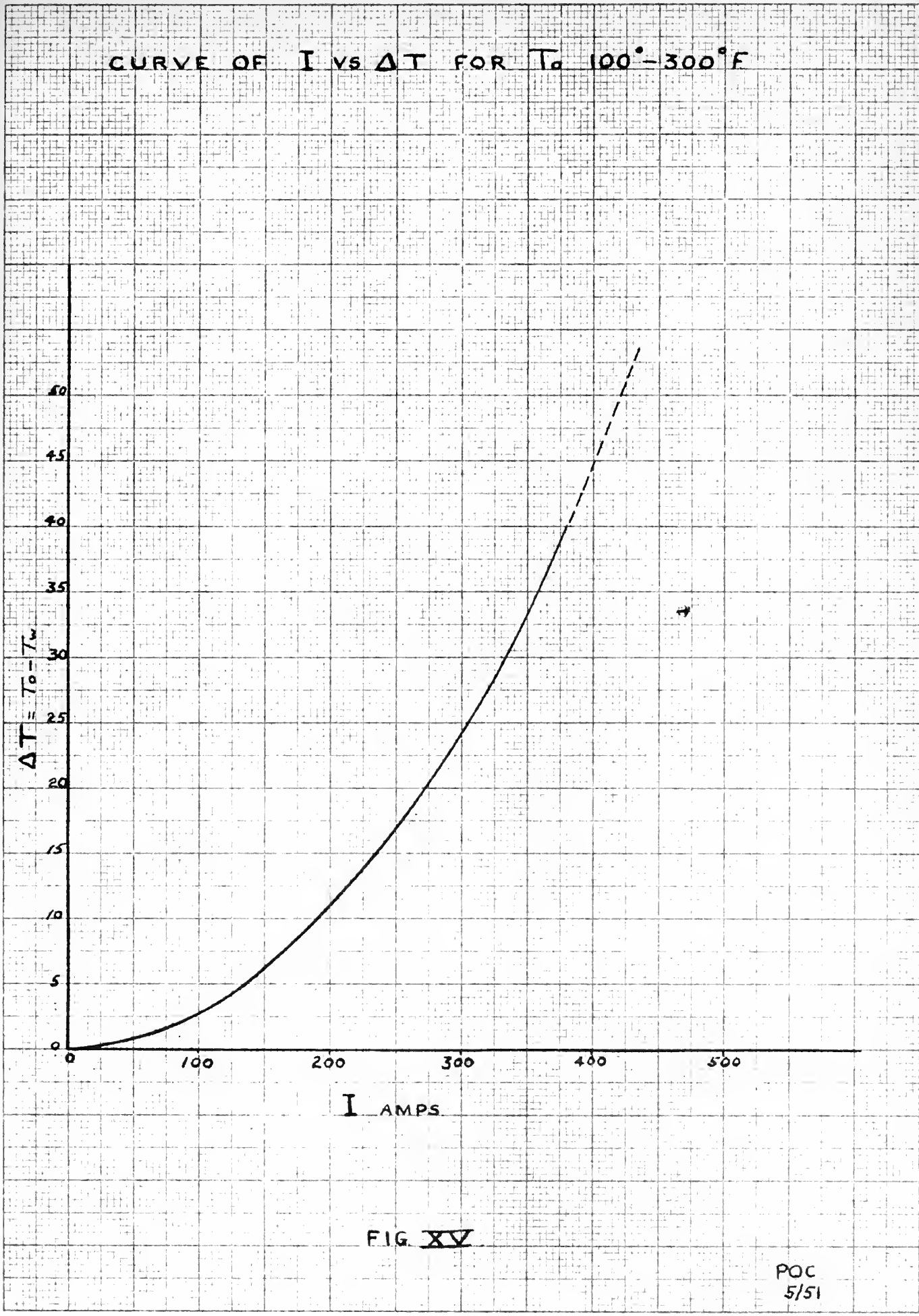

FIG. XV

POC
5/51

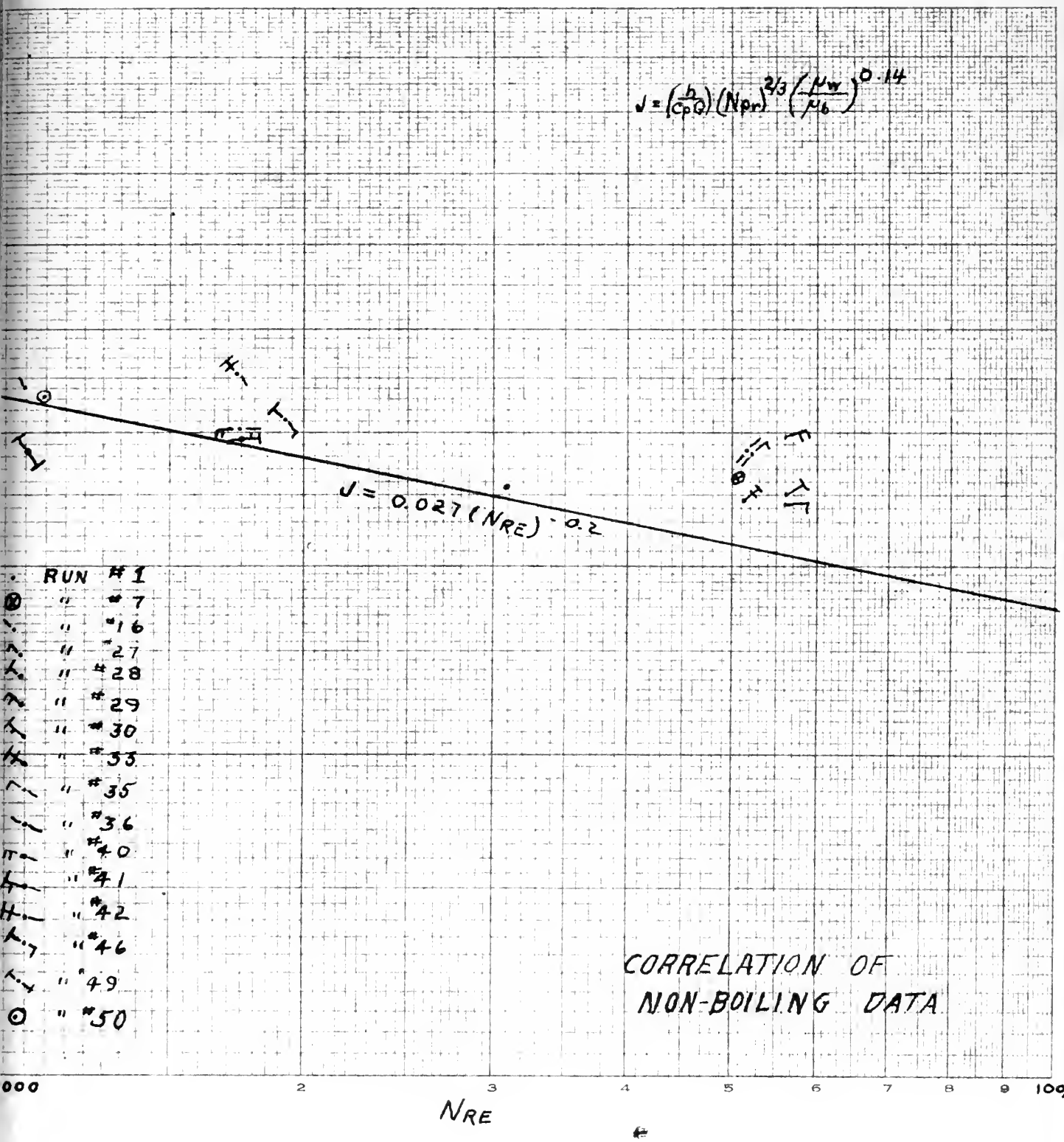

FIG. XVI

N.F.G.
5/51

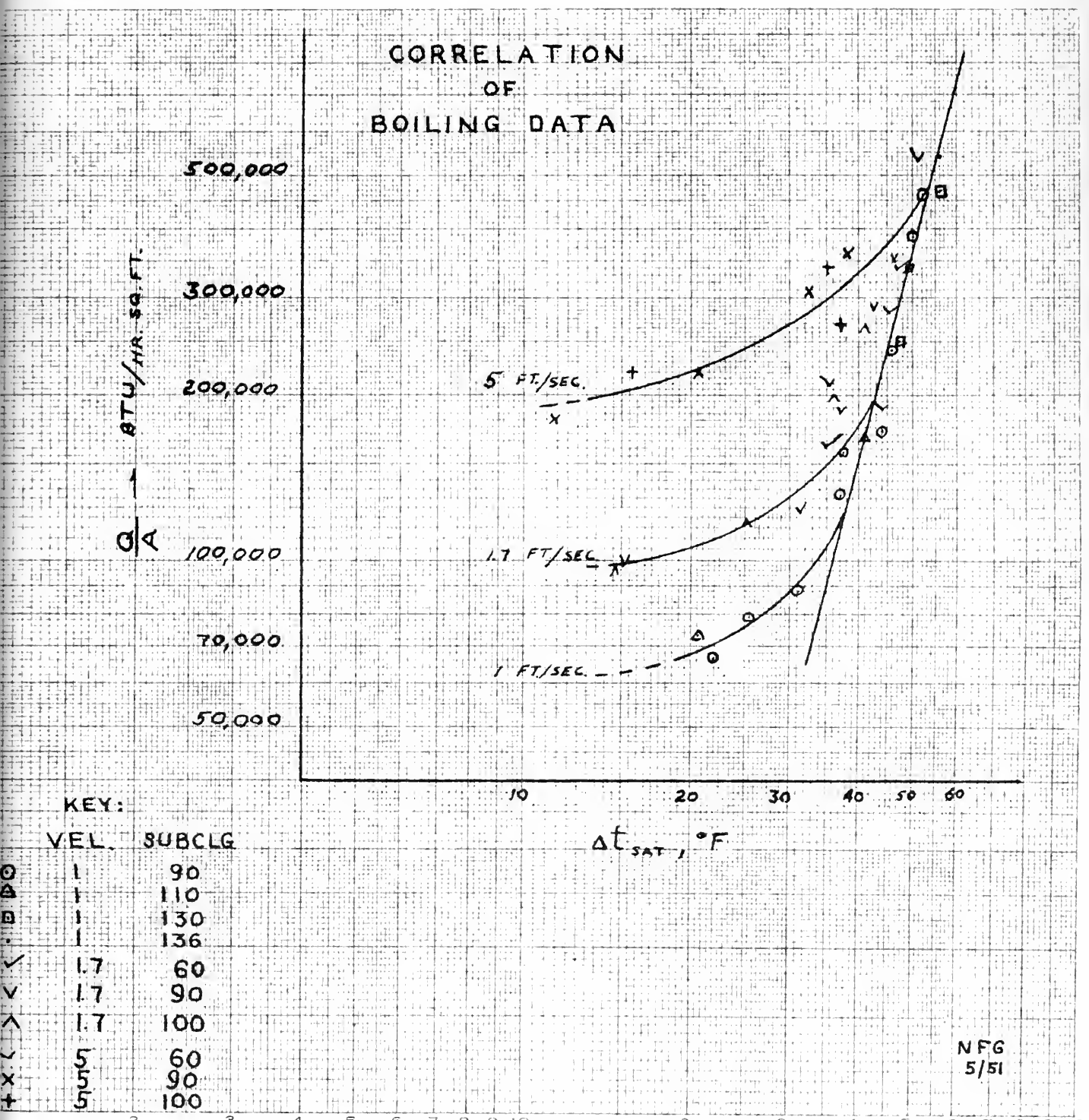
CORRELATION
OF
BOILING DATA
500,000
300,000
200,000
100,000
70,000
50,000
q/A — BTU/HR. SQ. FT.
5 FT./SEC.
1.7 FT/SEC.
1 FT/SEC.
10
20
30
40
50
60
Δt SAT, °F
KEY:
VEL. SUBCLG
1 90
1 110
1 130
1 136
1.7 60
1.7 90
1.7 100
5 60
5 90
5 100
NFG
5/51
2 3 4 5 6 7 8 9 10
2 3 4 5 6 7 8 9 10

FIG. XVII

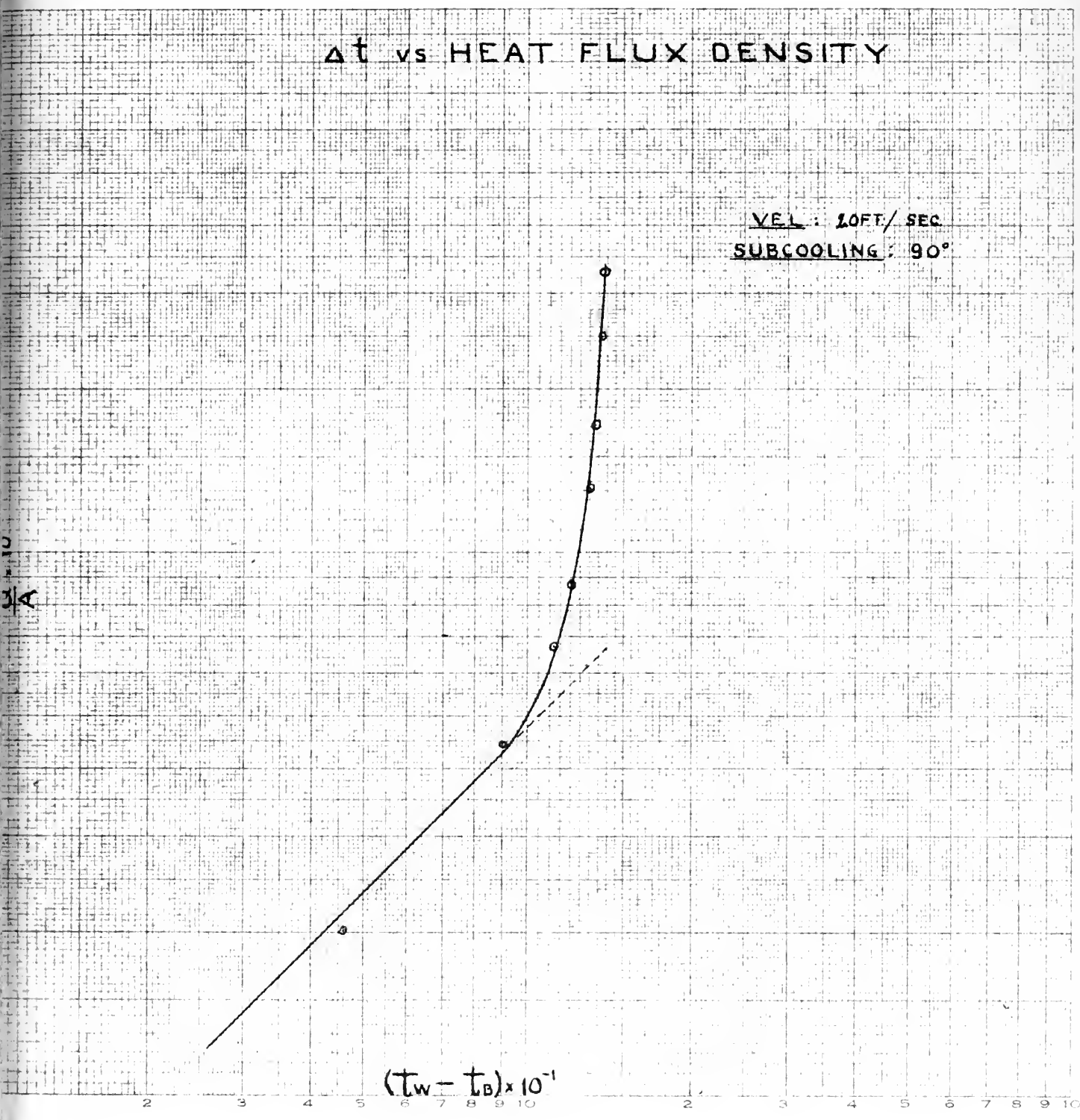

FIG. XVIII

POC
5/51

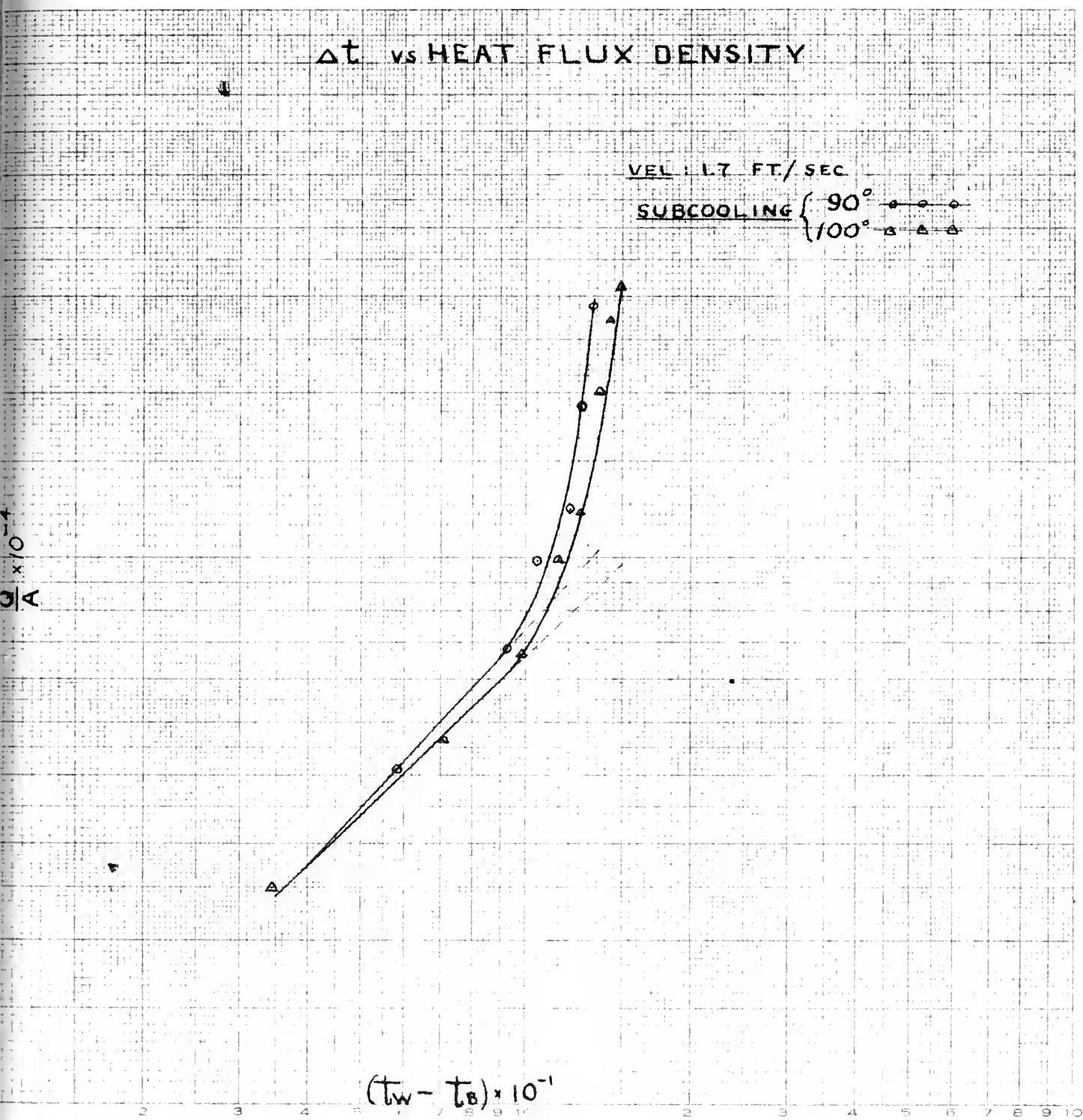

FIG. XIX.

POC
5/51

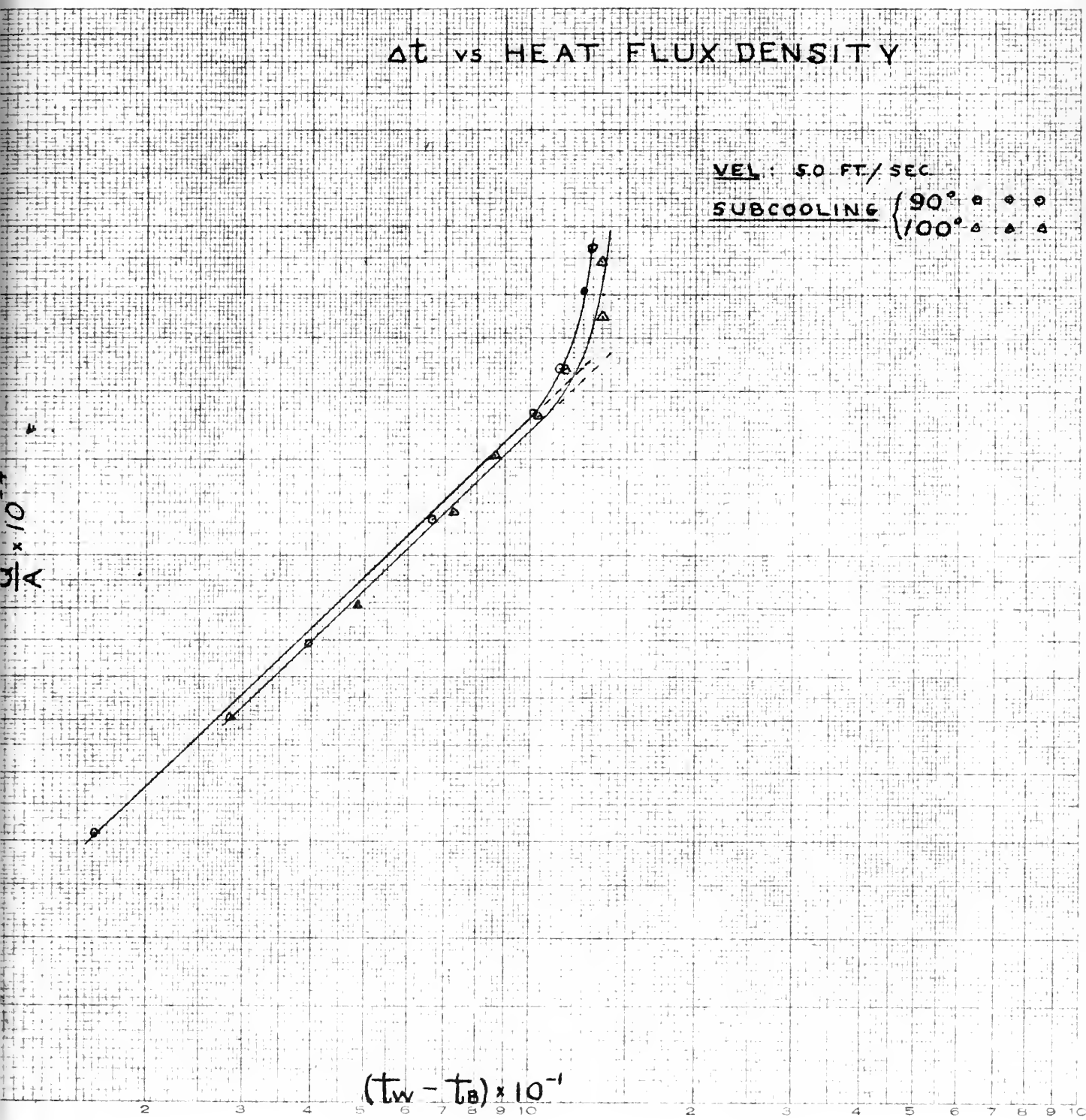

FIG XX

POC
5/51

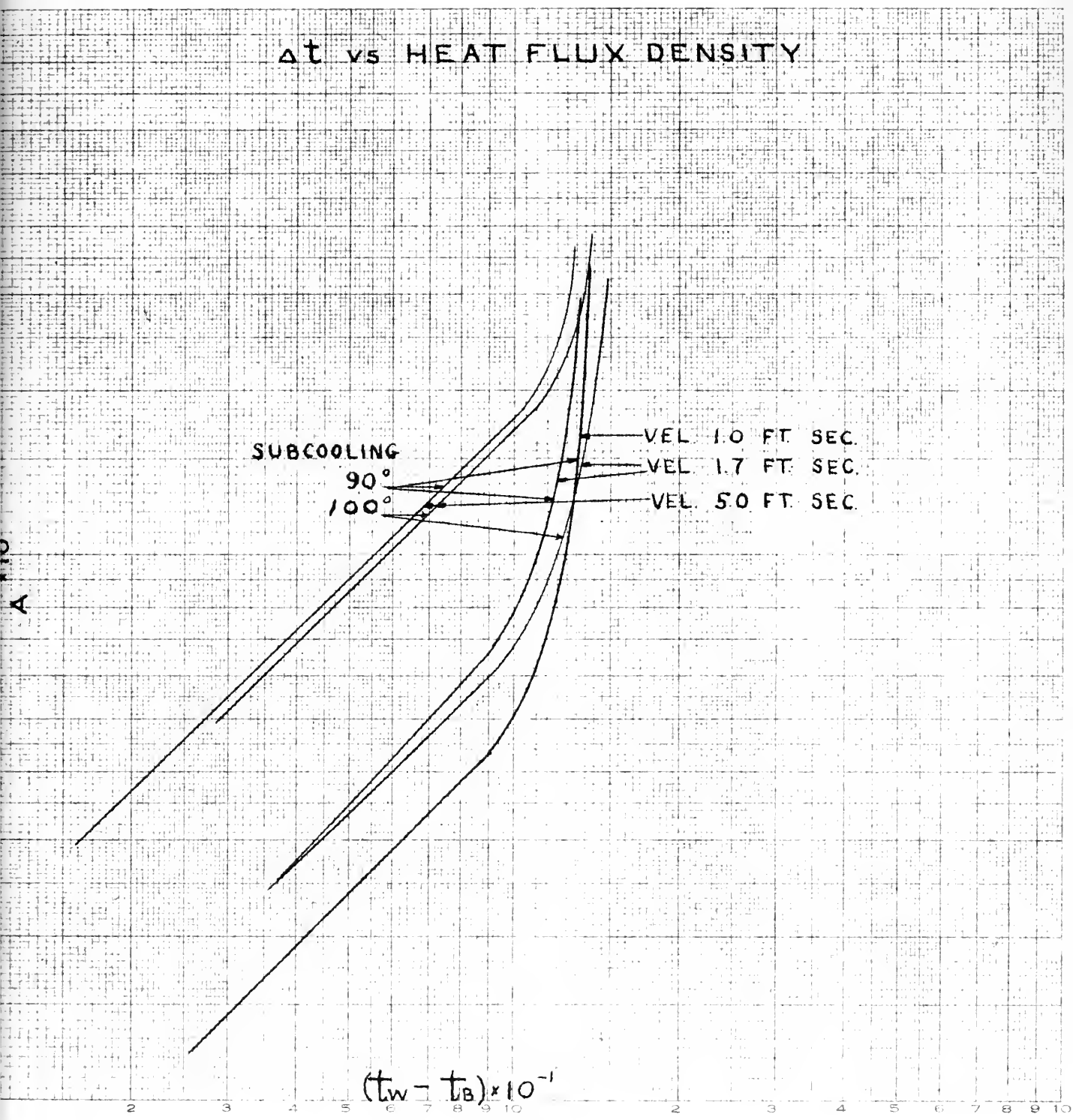

FIG. XXI.

POC
5/51

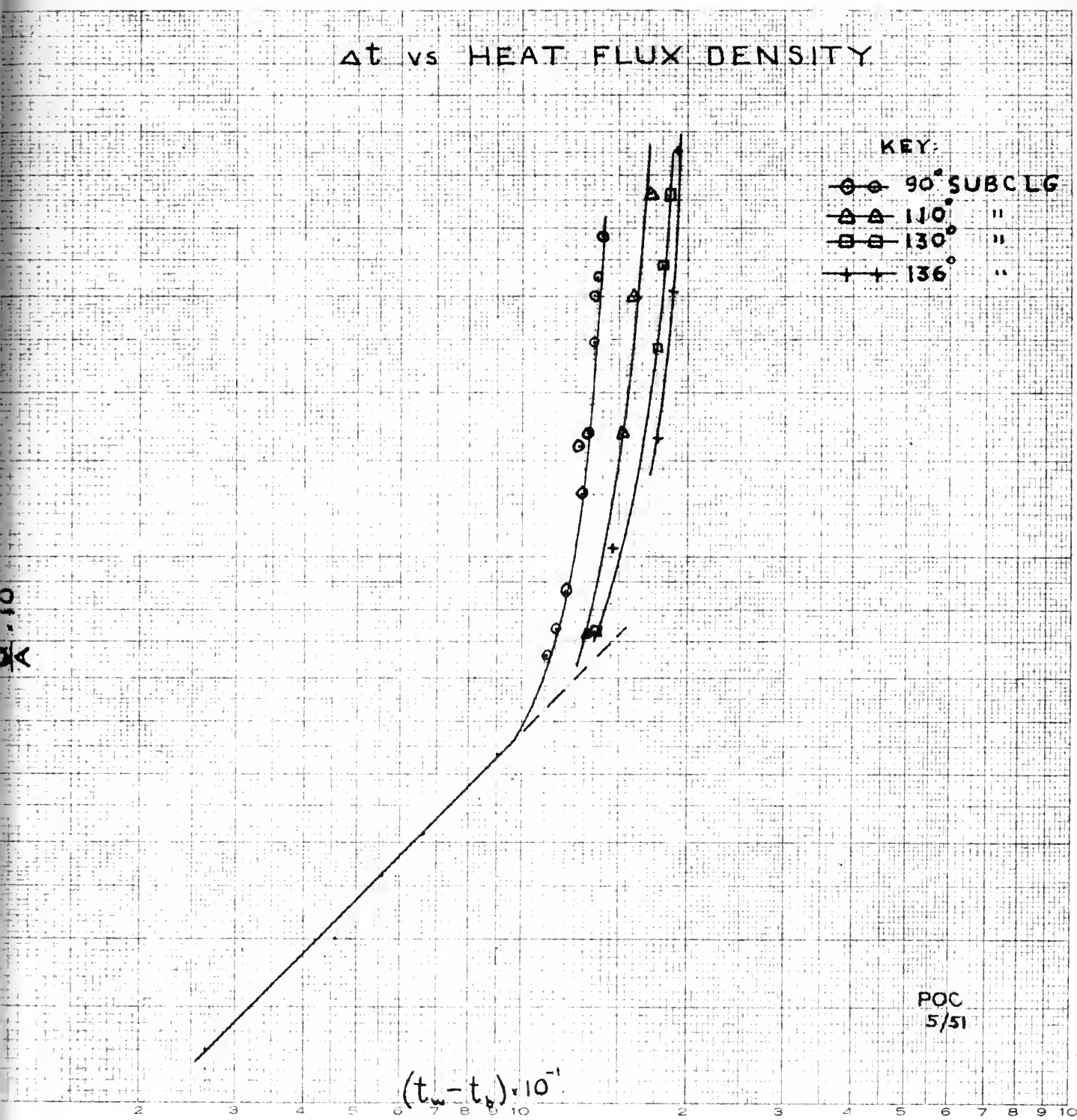
Δt vs HEAT FLUX DENSITY
KEY:
90° SUBC LG
110° "
130° "
136° "
POC
5/51
$(t_w - t_s) \cdot 10^{-1}$
2 3 4 5 6 7 8 9 10
2 3 4 5 6 7 8 9 10

FIG. XXII.

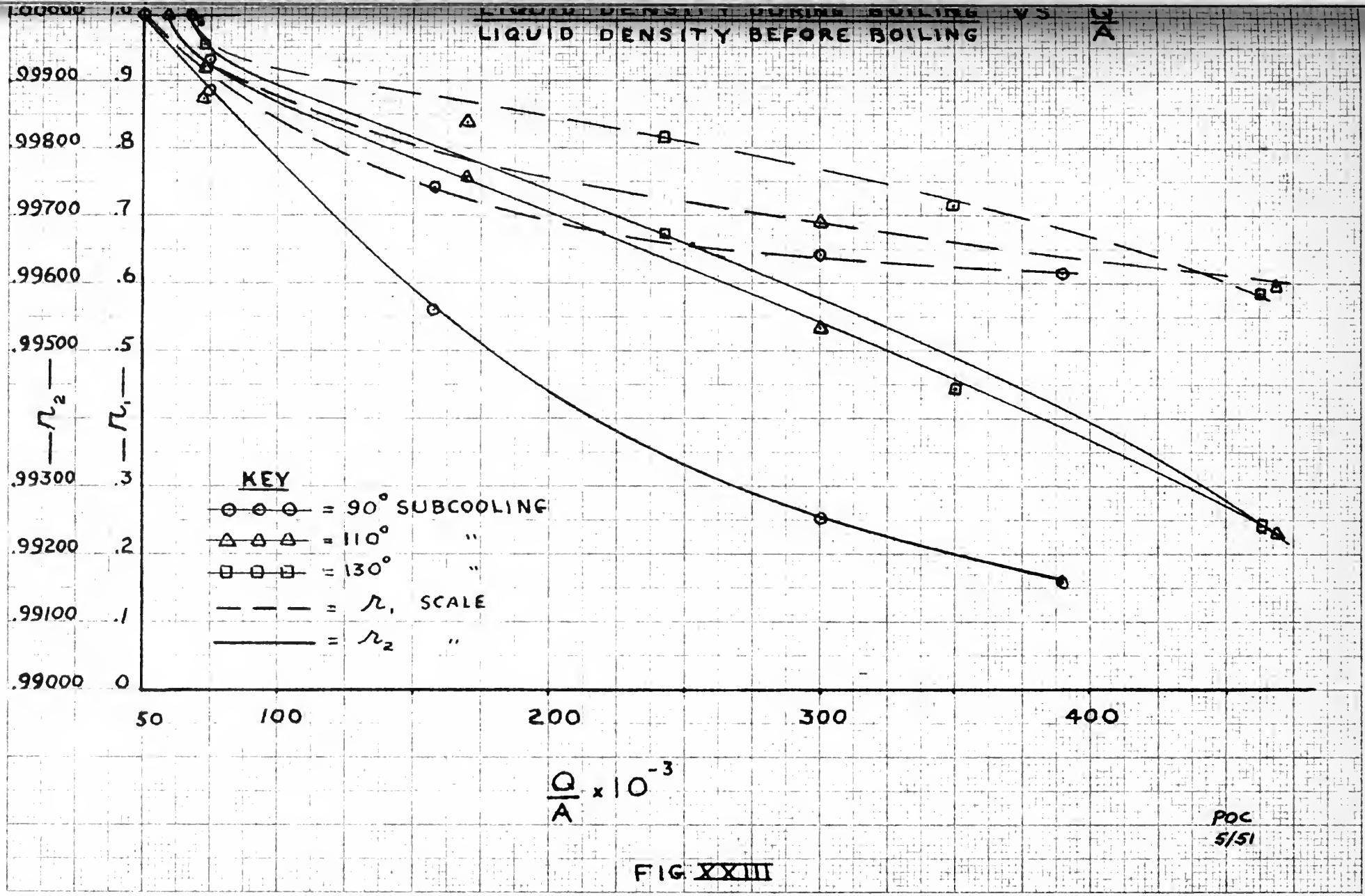

FIG XXIII

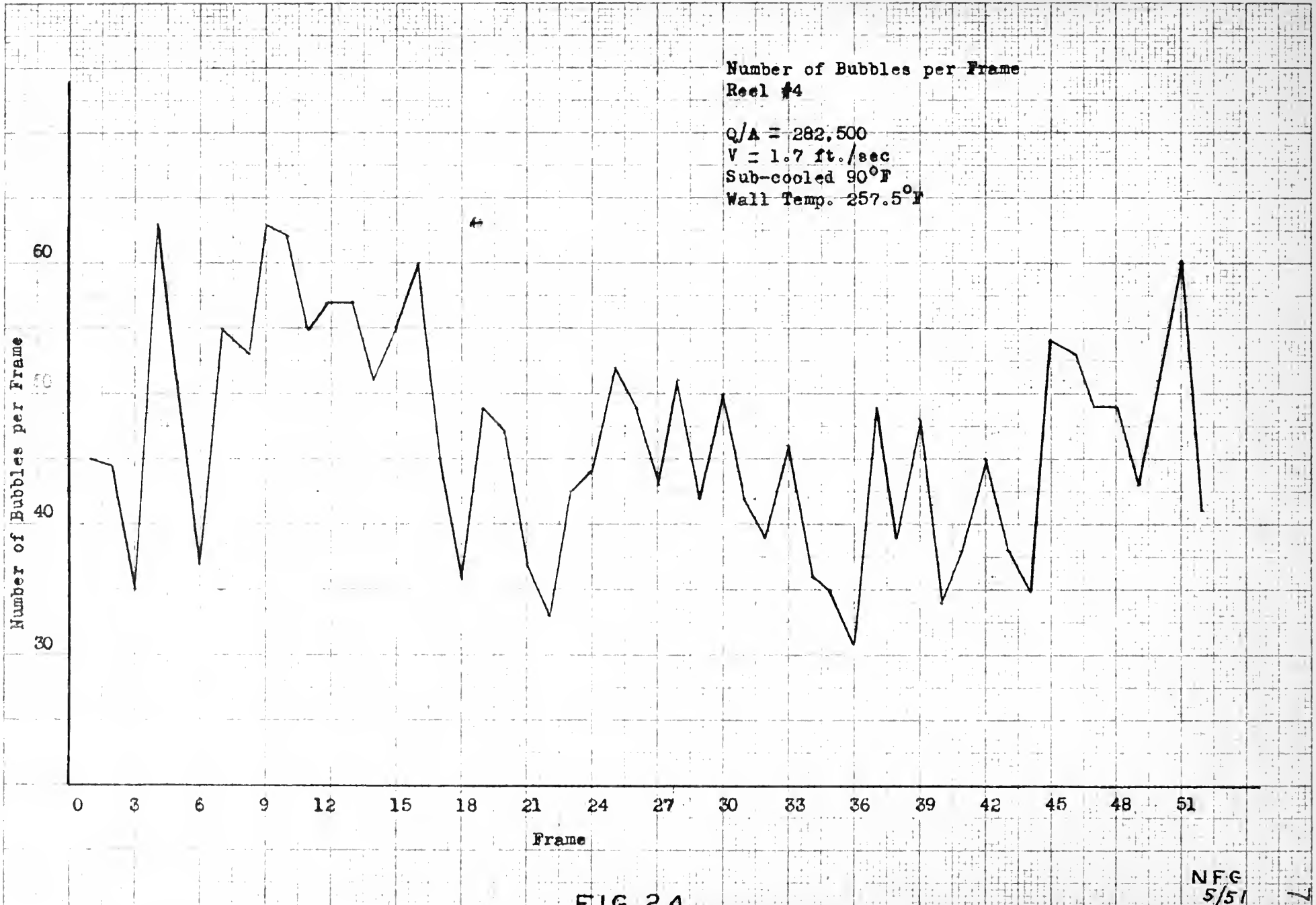

FIG. 24

NFG
5/51

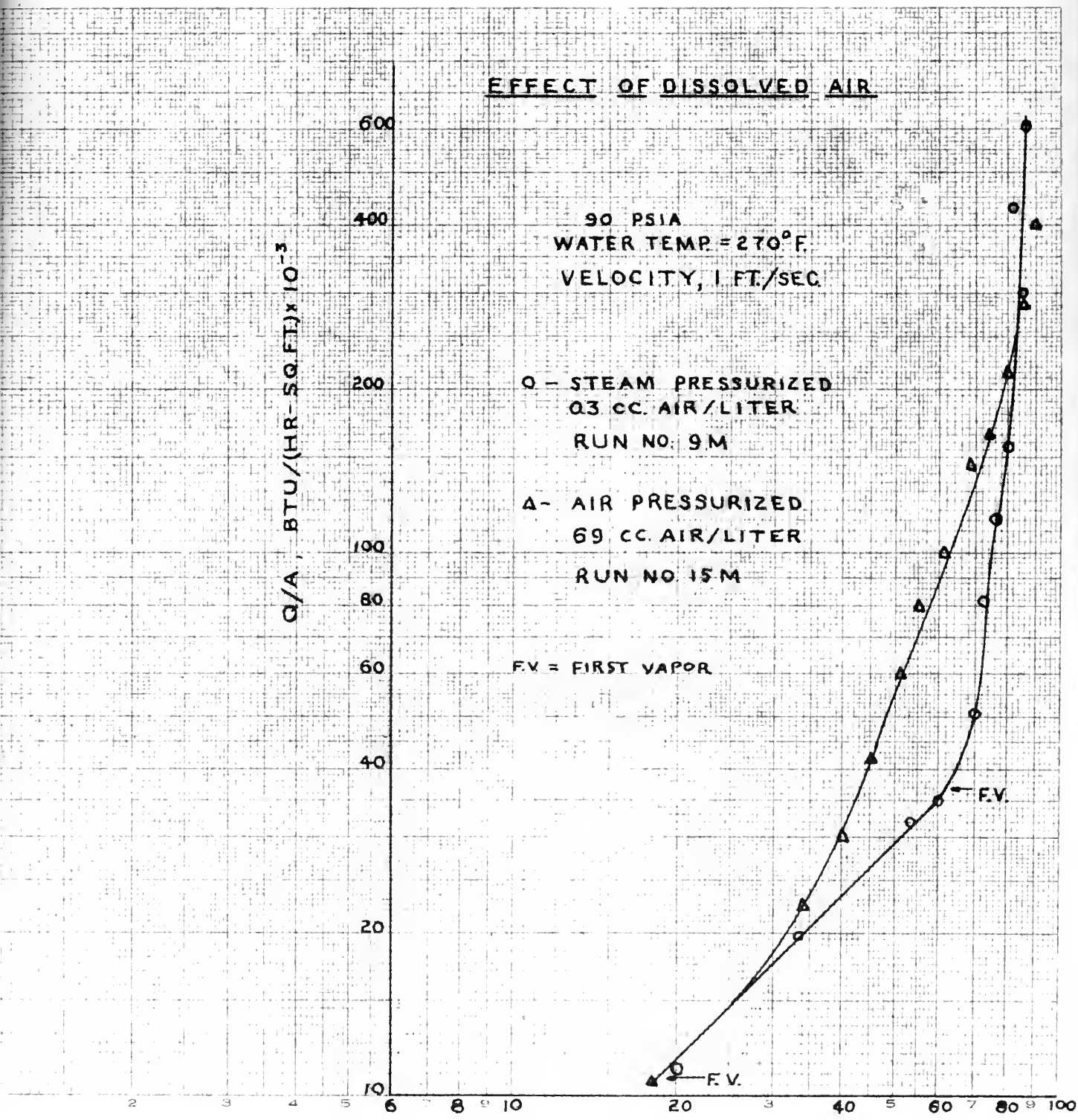

(5)/POC
5/61

FIG. XXV

COMPOSITE PHOTOGRAPH
TAKEN AT MEAN FLUID
VELOCITY OF 1 FT/SEC
SHOWING VARIATIONS
IN BUBBLE FORMATION
WITH HEAT FLUX DENSITY
AND SUBCOOLING

EXPOSURE TIME: 2×10^{-6} SECS.

FIG. XVII

COMPARISON PHOTOGRAPH

TAKEN AT MEAN FLUID

VELOCITY OF 1 FT/SEC

SHOWING VARIATIONS

IN SURFACE TEMPERATURE

WITH HEAT FLUX DENSITY

AND ABSCISSAE

EXPOSURE TIME: 3x10^{-6} SECS.

Run 58
$\frac{Q}{A}$ = 389,000
SubC.= 90°

Run 65
$\frac{Q}{A}$ = 467,000
SubC.= 110°

Run 66
$\frac{Q}{A}$ = 462,000
SubC.= 130°

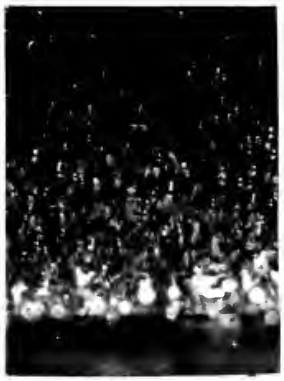

Run 70
$\frac{Q}{A}$ = 545,000
SubC.= 136°

Run 59
$\frac{Q}{A}$ = 301,000
SubC.= 90°

Run 64
$\frac{Q}{A}$ = 300,000
SubC.= 110°

Run 67
$\frac{Q}{A}$ = 347,000
SubC.= 130°

Run 71
$\frac{Q}{A}$ = 306,000
SubC.= 136°

Run 60
$\frac{Q}{A}$ = 158,000
SubC.= 90°

Run 63
$\frac{Q}{A}$ = 169,000
SubC.= 110°

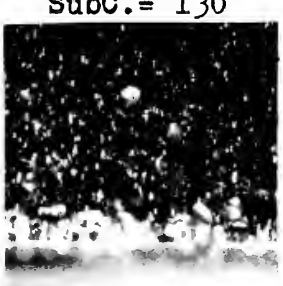

Run 68
$\frac{Q}{A}$ = 242,000
SubC.= 130°

Run 72
$\frac{Q}{A}$ = 165,000
SubC.= 136°

Run 61
$\frac{Q}{A}$ = 74,250
SubC.= 90°

Run 62
$\frac{Q}{A}$ = 72,500
SubC.= 110°

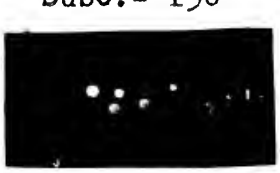

Run 69
$\frac{Q}{A}$ ≠ 72,700
SubC.= 130°

Run 73
$\frac{Q}{A}$ ≠ 103,500
SubC. = 136°

COMPOSITE PHOTOGRAPH

SHOWING VARIATION

IN BUBBLE POPULATION

WITH HEAT FLUX DENSITY

AT DIFFERENT VELOCITIES

BUT HAVE Δt_{sat}.

EXPOSURE TIME: 3×10^{-3} SEC.

FIG. XVIII.

CHROMOSOME CHOLOGENESIS

SHOCKING VARIATION

IN SHARPLY MORNINGLY

WICK NEAT TICK DENSITY

AT DIFFERENT ACCOMPLISHED

BUT DARK $\Delta^{8\pi\zeta}$.

EXPLODING CINE: DARK_SHADE.

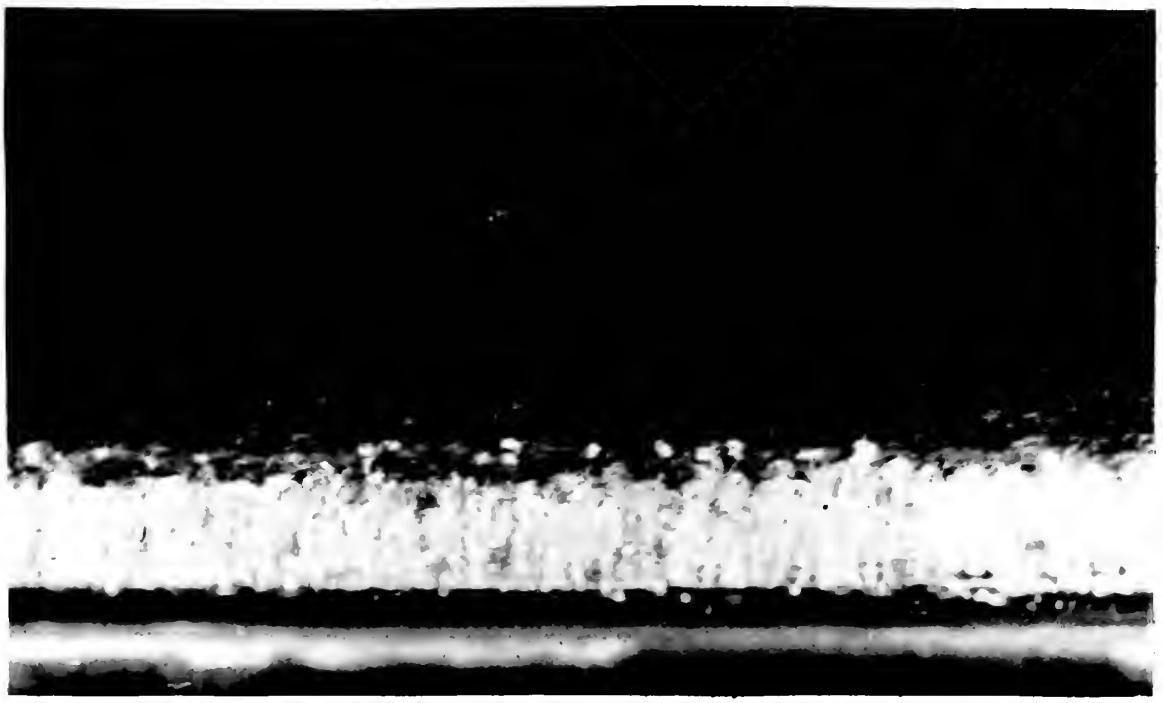

Run #19 - Picture #4
Q/A = 161,800; t_{sat} = 35°F. t_b = 148°F.
Velocity = 1.7 Ft./Sec.

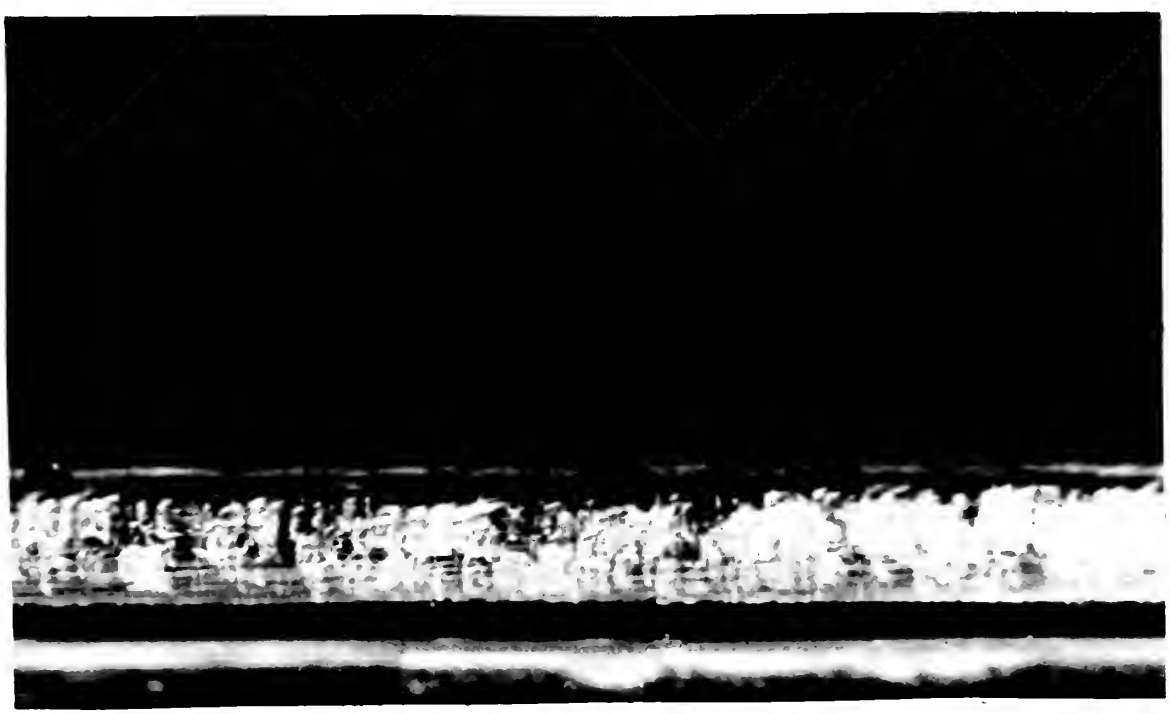

Run #23 - Picture #8
Q/A = 205,700; t_{sat} = 35.5°F. t_b = 150.5°F.
Velocity = 5 Ft/Sec.